Infliximab was given intravenously over 2 h at a dose of 5 mg/kg on 0, 2, and 6 weeks, with follow-up treatments every 7–8 weeks depending on clinical symptoms. The patient was monitored regularly throughout the infliximab treatment.

Results

Case

The patient was born to unrelated Japanese parents after an uncomplicated pregnancy of 41 weeks. There was no history of any first-degree relative diagnosed with incontinentia pigmenti. On the first day after birth, he presented high fever with a markedly increased white blood cell count ($40\times10^3/\mu L$) and was treated successfully with antibiotics. He has had a history of recurrent, severe infections including varicella at 3 months of age, penicillin-resistant *Streptococcus pneumoniae* meningitis at 6 months of age, and zoster at 8 months of age. Persistent diarrhea was also observed.

He was introduced to our hospital at 8 months of age for examination of his immunological status. On admission, he showed a marked increase in both white blood cells ($31.9\times10^3/\mu L$) and platelets ($872\times10^3/\mu L$). Peripheral blood T cell count was decreased (CD3-positive cells, 25.8%), and B cell count was highly increased (CD20-positive cells,: 69.2%). PHA induced a normal proliferation response of T cells, and concentrations of immunoglobulins were within the normal range except IgD (less than 0.2 mg/dL). Natural killer cell activity was markedly impaired. Superoxide-generating ability from neutrophils was intact. LPS-induced TNFα production from patient's PBMC was impaired (Fig. 1a). Interferon (IFN) γ-producing lymphocytes were also reduced apparently at 8 months of age (Table I). All the genes involving in the IL-12 signal pathway, including *IL12RB1*, *IL12RB2*, *JAK2*, and *STAT4* were sequenced, but no mutations were found (data not shown). Surprisingly, both IFNγ-producing T cells and natural killer cells had expanded significantly by 11 months of age (Table I). In addition, we observed that he had ectodermal dysplasia including anhidrosis and conical teeth (Supplementary Fig. 1). A skin biopsy revealed the absence of eccrine sweat glands. When he was 3 years old, a G505C (A169P) missense mutation in his *IKBKG* gene was confirmed and diagnosed as X-EDA-ID. His mother was a carrier. An expression of mutant NEMO protein was not markedly

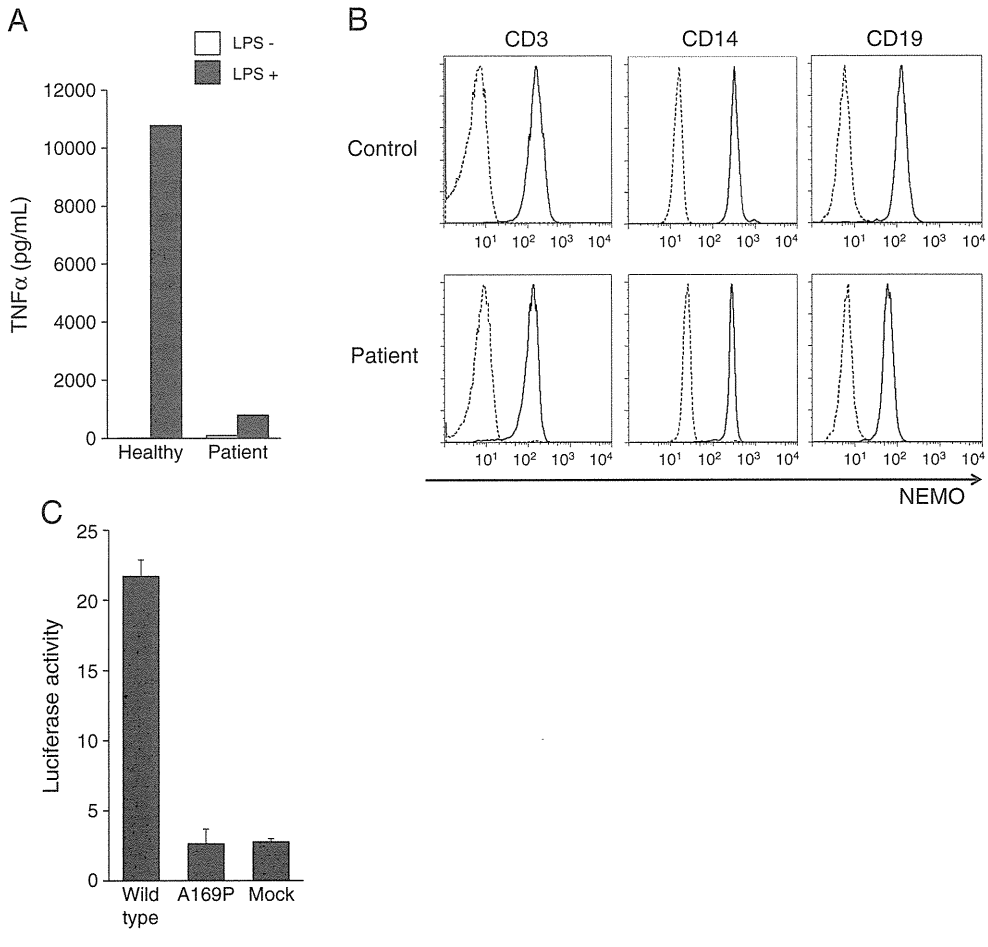

Fig. 1 Analysis of mutant NEMO protein. **a** Reduced production of TNFα from LPS-stimulated PBMCs. PBMCs from our patient and healthy volunteer were stimulated with LPS (1 μg/mL). **b** Analysis of NEMO protein expression using flow cytometry. Intracellular NEMO protein in PBMCs from the patient was not reduced markedly. **c** The result of NEMO-NF-κB luciferase reporter assay. The activity of mutant NEMO in the patient was almost defective. Mock vectors and wild-type NEMO were used as controls. *Error bars* indicate SD

Table I Proportion of IFNγ-expressing T and NK cells in the patient

Age	$IFN\gamma^+/IL\text{-}4^-$		
	CD4 (%)	CD8 (%)	CD56 (%)
8 months	1.14	8.83	2.00
11 months	3.18	70.40	66.29
3 years 11 months	11.89	65.48	82.79
Healthy control	15	60–80	80–90

reduced by flow cytometer (Fig. 1b), but the activity of mutant NEMO was almost defective which was confirmed by a mutant NEMO-NF-κB luciferase reporter assay (Fig. 1c). He has been prescribed prophylactic cotrimoxazole before and after the diagnosis.

He presented with chest pain, erythema, polyarthritis, continuous high fever refractory to antibiotics, and marked elevation of C-reactive protein (7.4 mg/dL) at 4 years of age. Autoantibodies such as anti-centromere antibody were detected transiently. Chest computed tomography revealed multiple nodular shadows resembling bronchiolitis obliterans organizing pneumonia. The repertoire of T cell receptor showed high expression of limited Vβ subsets (Supplementary Fig. 2). Combination therapy using corticosteroids, cyclosporine A, and methotrexate was effective and was continued to control his symptoms.

Severe abdominal pain and intractable frequent diarrhea recurred when the corticosteroid dose was reduced, and he presented perianal fistula at 8 years of age. A mild elevation was observed in both erythrocyte sedimentation rate and C-reactive protein under the preceding immunosuppressive treatments (Table II). No significant pathogen was detected by stool culture and the use of antibiotics and antifungal drugs resulted in no improvement in clinical symptoms.

Endoscopic and Microscopic Findings of the Colon

Colonic endoscopy revealed many polyp-like lesions with mucosal redness and edema at the sigmoid/descending junction (Fig. 2). A longitudinal ulcerative lesion found in the sigmoid colon was suggestive of Crohn's disease. Passing the endoscope beyond these obstructive clusters of polyps was difficult; therefore, we could not observe the upper part of the colon. Neither stenosis nor ulcer formation was observed by intestinal radiocontrast analysis.

Histopathological examination of the colonic biopsied specimens showed diffuse lymphoplasmacytic infiltration, superficial edema, and hyperemia in lamina propria. Foamy cells and some eosinophils were also seen (Fig. 3a, b). No definite neutrophilic infiltration, crypt abscesses, or granulomatous lesions were observed. Cultures from biopsied specimens yielded neither bacterial nor fungal growth.

Immunohistochemical staining revealed predominant infiltration of CD79a-positive, plasma cells in the lamina propria. Infiltration of CD68-positive macrophages and CD3-positive T cells was also observed (Fig. 3c–g).

Detection of TNFα-Producing Cells in the Lamina Propria and Peripheral Blood

To investigate the possibility that TNFα blockade therapy can ameliorate inflammatory colitis as well as NEMO-deficient mice as suggested by previous analysis [15], we analyzed TNFα-producing mononuclear cells in the lamina propria in the colon of our patient. Immunohistochemical staining showed abundant TNFα in infiltrated mononuclear cells in the lamina propria (Fig. 3h) which would be associated with progression of inflammatory colitis.

We also analyzed TNFα-producing T cells and monocytes in the peripheral blood (Fig. 4a). The majority (72.49%) of CD4-positive T cells in our patient expressed intracellular TNFα, while 40% to 70% of CD4-positive T cells expressed TNFα in adults with IBD in our study. Forty-eight percent of CD8-positive T cells in our patient expressed TNFα. CD14-positive monocytes from our patient expressed small amounts of intracellular TNFα after LPS stimulation, while similarly treated CD14-positive cells from healthy subjects expressed abundant TNFα (Fig. 4b).

Reversion Analysis

Nishikomori et al. reported that in an X-EDA-ID patient, the mutation had been reverted to the normal state in IFNγ-

Table II Laboratory data on admission (8 years old)

WBC	13,600/μL	CD3	76.2%	IgG	790 mg/dL
Neutrophils	10,200/μL	CD4	22.2%	IgA	666 mg/dL
Lymphocytes	1,632/μL	CD8	58.3%	IgM	71 mg/dL
Monocytes	952/μL	CD19	4.8%	IgD	<0.6 mg/dL
Hemoglobin	12.0 g/dL	CD20	3.8%	C3	134 mg/dL
Platelets	84.7×10^4/μL	CD16	0.5%	C4	46 mg/dL
		CD56	33.6%	CH50	56 U/mL
		HLA-DR	26.5%	ESR	43 mm/h

WBC white blood cell, *CH50* total complement activity, *ESR* erythrocyte sedimentation rate

Fig. 2 Findings of colonoscopy performed before initial treatment with infliximab. Colonoscopy revealed polyp-like lesions with mucosal redness and edema at the sigmoid/descending junction (*left panel*). A longitudinal ulcer (*arrowhead*) was found in the sigmoid colon (*center panel*). Same segment as in the *center panel* after indigo carmine dye (*right panel*)

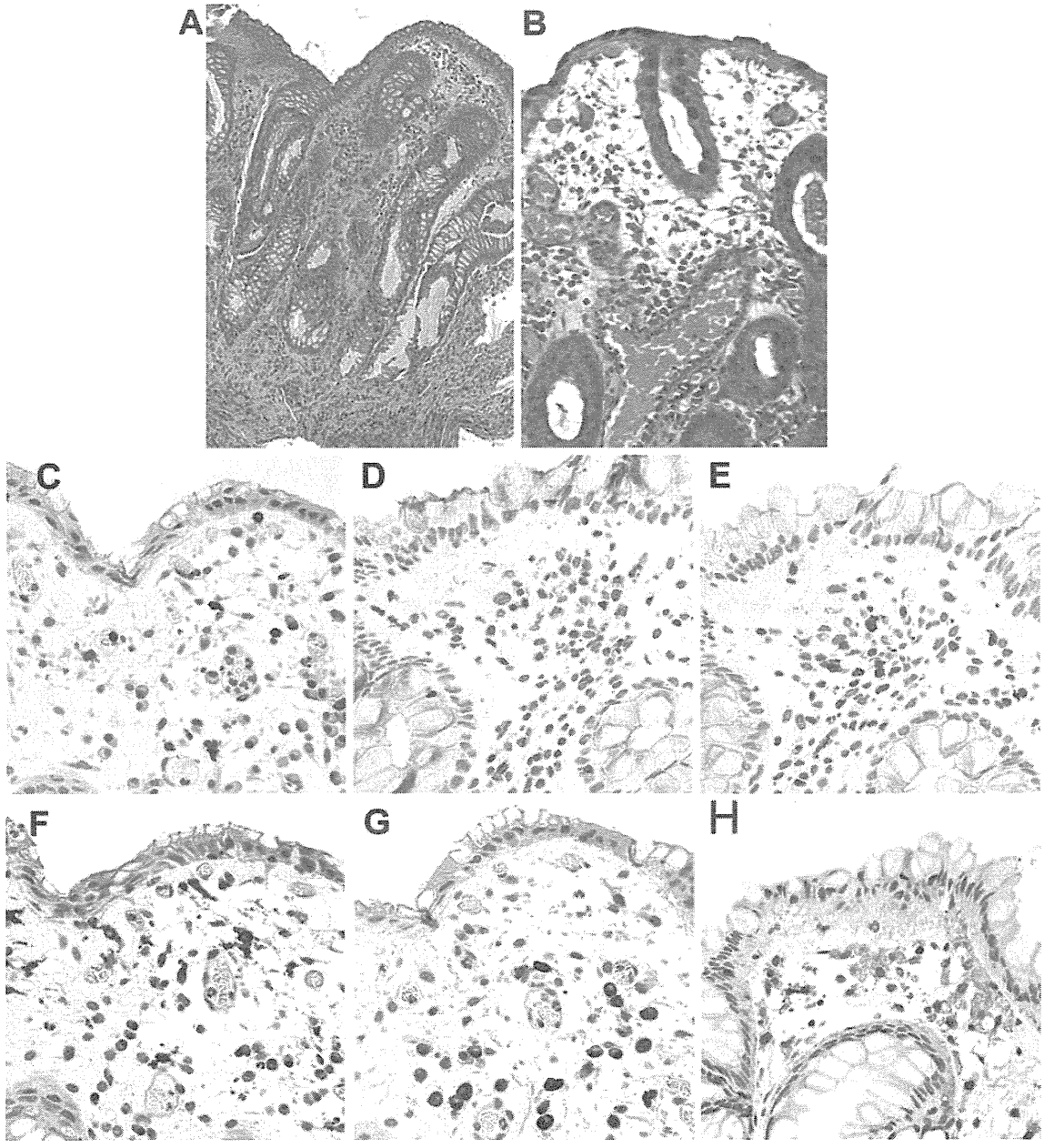

Fig. 3 Microscopic findings of affected colonic specimens. **a**, **b** Hematoxylin and eosin staining. **a** and **b** are low-power field and high-power field views, respectively. **c**–**h** Staining profiles of cellular surface antigens: **c** CD3ε, **d** CD4, **e** CD8, **f** CD68, and **g** CD79a. **h** Staining with anti-human TNFα antibody

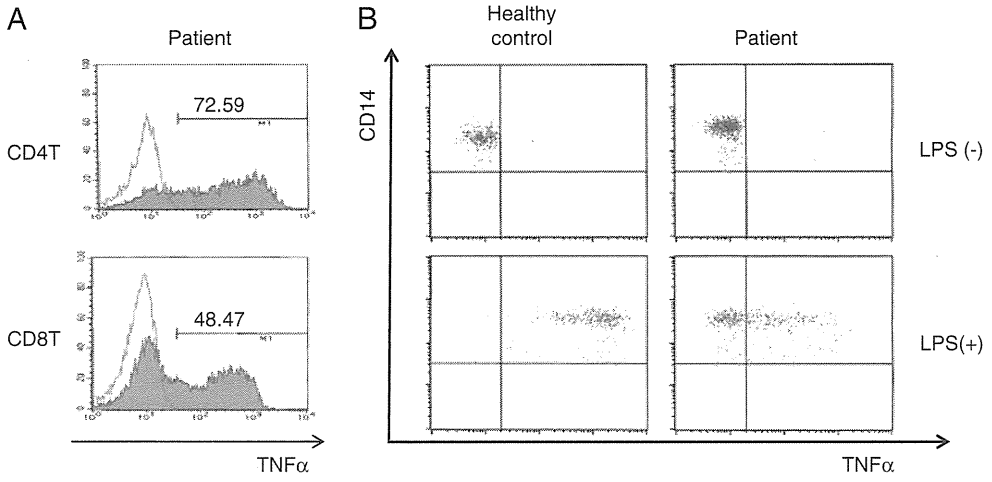

Fig. 4 Analysis of TNFα-producing mononuclear cells in peripheral blood. **a** TNFα-expressing T cells increased markedly before infliximab treatment. PBMCs were stimulated with ionomycin and PMA for 4 h in the presence of brefeldin A then stained for intracellular TNFα. For FACS analysis, gates were set on lymphocytes according to forward and side scatter properties. Representative histograms of TNFα expression in stimulated (*solid histograms*) or unstimulated (*black line histograms*) T cells. The proportion of TNFα-positive CD4-positive T cells in adult IBD patients is 40–70%. **b** The percentage of TNFα-positive monocytes was examined. Cells from our patient and healthy volunteer were incubated with or without LPS for 4 h in the presence of brefeldin A. Monocytes were identified by CD14. Approximately 50% of stimulated monocytes produced a small amount of TNFα

expressing T cells [18]. Our patient showed expansion of IFNγ-expressing T cells during infancy and an increase in TNFα-producing T cells at that time. We hypothesized that the A169P mutation in the *IKBKG* gene had been reverted to wild type and that the reverted T cells had expanded in our patient. Indeed, before initiating infliximab treatments, reversion mutation was detected in 23/67 (34%) from non-stimulated PBMCs (Table III). At 24 months after the initiation, reversion mutation was detected in both messenger RNA (mRNA) and genomic DNA from lymphocytes stimulated with PHA and IL-2 for 10 days, whereas only mutated mRNA was identified from non-stimulated lymphocytes (Fig. 5). Reverted mRNA was observed in CD3-positive T cells. Sex chromosome analysis with fluorescent in situ hybridization revealed no maternal cells and therefore graft-versus-host disease secondary to maternal–fetal transfusion was unlikely. These findings suggest that reverted T cells activated NF-κB in response to growth signals and had a growth advantage over mutant cells.

Table III Frequency of reverted clones before and after initiation of infliximab treatments

	Before	After 12 months	After 24 months
PBMCs	23/67 (34%)	nd	2/6 (33%)[a]
CD3	nd	3/16 (19%)	nd
CD14	nd	0/19 (0%)	nd
CD19	nd	0/47 (0%)	nd

nd not done

[a] A result using stimulated mononuclear cells

Reverted T cells decreased with repeated administrations of anti-TNFα monoclonal antibody. In contrast, CD14-positive monocytes and GM-CSF-induced monocyte-derived dendritic cells had no reversion (Table III).

Anti-TNFα Treatment Improved NEMO Colitis

We initially treated NEMO colitis with high dose corticosteroid therapy (2 mg/kg prednisolone, daily) (Fig. 6). However, steroid therapy did not improve clinical symptoms and resulted in compression fracture in the thoracic spine from corticosteroid-induced osteoporosis.

The increase in TNFα-producing T cells suggested the possibility that TNFα blockade therapy would be an effective treatment for the intractable NEMO colitis. After confirming the absence of severe bacterial or mycobacterial infection, we initiated administration of the chimeric anti-TNFα monoclonal antibody, infliximab, to our patient.

Soon after the first infusion of infliximab, abdominal pain disappeared and his appetite recovered. Frequency of diarrhea decreased as administrations of infliximab were repeated (Fig. 6). Colonoscopy after his third administration showed mild improvement of both mucosal redness and edema (Fig. 7a). These mucosal inflammatory findings had almost disappeared after 1-year treatment with infliximab, although polyp-like lesions remained (Fig. 7b).

The proportion of TNFα-producing cells in CD4-positive and CD8-positive T cells markedly decreased by his third infliximab infusion (from 72.6% to 26.7% in CD4-positive T cells and from 48.5% to 23.1% in CD8-positive T cells), and reduction of TNFα-producing cells was

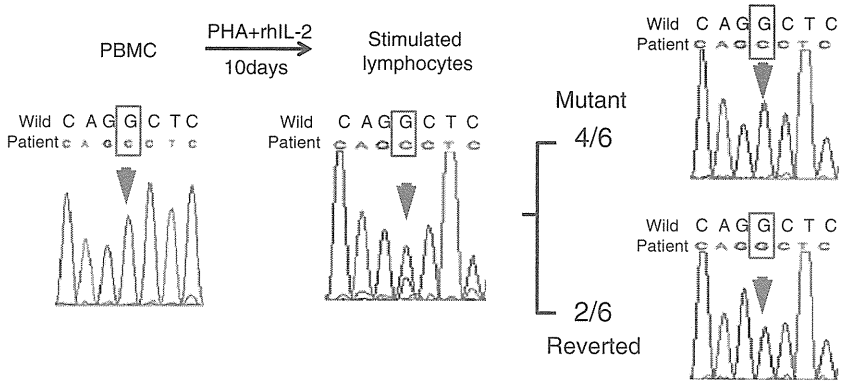

Fig. 5 Reversion analysis of cDNA of gene encoding NEMO isolated from mononuloclear cells after 24 months of infliximab treatment. PBMC was obtained from our patient and incubated with PHA and IL-2 for 10 days. Direct sequence for mRNA encoding NEMO was performed using PBMC and the stimulated mononuclear cells. Before stimulation, no reverted mononuclear cells were detected. After PHA and IL-2 stimulation, reverted mononuclear cells apparently increased. Subcloning of cDNA from stimulated cells showed that two of six cells had reversion of mutation in the gene

associated with improvement of clinical symptoms (Fig. 6). Administration of cyclosporine A was discontinued by the eighth infliximab treatment, and corticosteroid was reduced and then discontinued by the tenth infliximab infusion.

Our patient had one serious adverse event, pneumonia, after his fourth administration of infliximab. *Campylobacter jejuni* was isolated from his blood culture at that time. He was successfully treated with antibiotics and infliximab administration was resumed after confirming resolution of pneumonia. He has been treated safely for more than 2 years with regular administrations of infliximab (once every 7–8 weeks). Neither mycobacterial infections nor severe infusion reactions have been observed.

Discussion

Our patient showed immunodeficiency with very low IFNγ-production during his younger years as shown in Table I and suffered from many opportunistic infections (Zoster virus infection, penicillin-resistant *Streptococcus pneumoniae* meningitis, and other undetermined infections). A novel missense mutation, A169P, in the first coiled-coil domain resulted in defective NEMO function (Fig. 1) and was responsible for recurrent severe infections. However, he later suffered from autoimmune diseases at 4 years of age (bronchiolitis obliterans organizing pneumonia, severe arthritis, and vasculitis) and severe chronic inflammatory colitis at 8 years. Based on the facts that, in the mice model, TNFα played a major role in the pathogenesis of NEMO colitis [15], and that, in our patient, TNFα-producing mononuclear cells in the peripheral blood were markedly increased (Fig. 4a), infliximab was employed for the patient's treatment. This treatment led to improvement in his symptoms and colonoscopic findings for 2 years.

Increases in TNFα-producing cells similar to that seen in other IBD [19] were detected (Fig. 4). We confirmed G/C

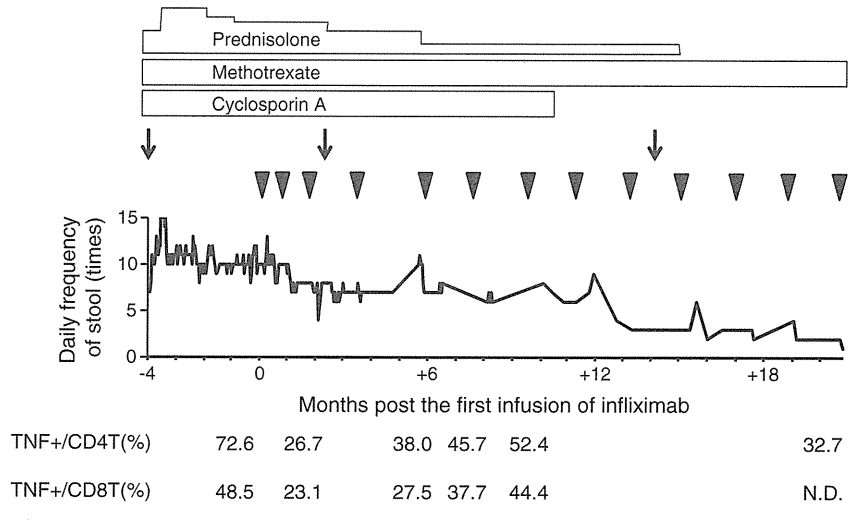

Fig. 6 Clinical course of NEMO colitis after infliximab treatment in our patient. Colonoscopy (*arrows*), administrations of infliximab (*arrowheads*), and other immunosuppressive drugs (*bars*) are indicated. Daily frequency of stools (times) is graphed at the *center*. Changes in the proportion of TNFα-producing T cells in CD4-positive and CD8-positive cells are also indicated at the *bottom*

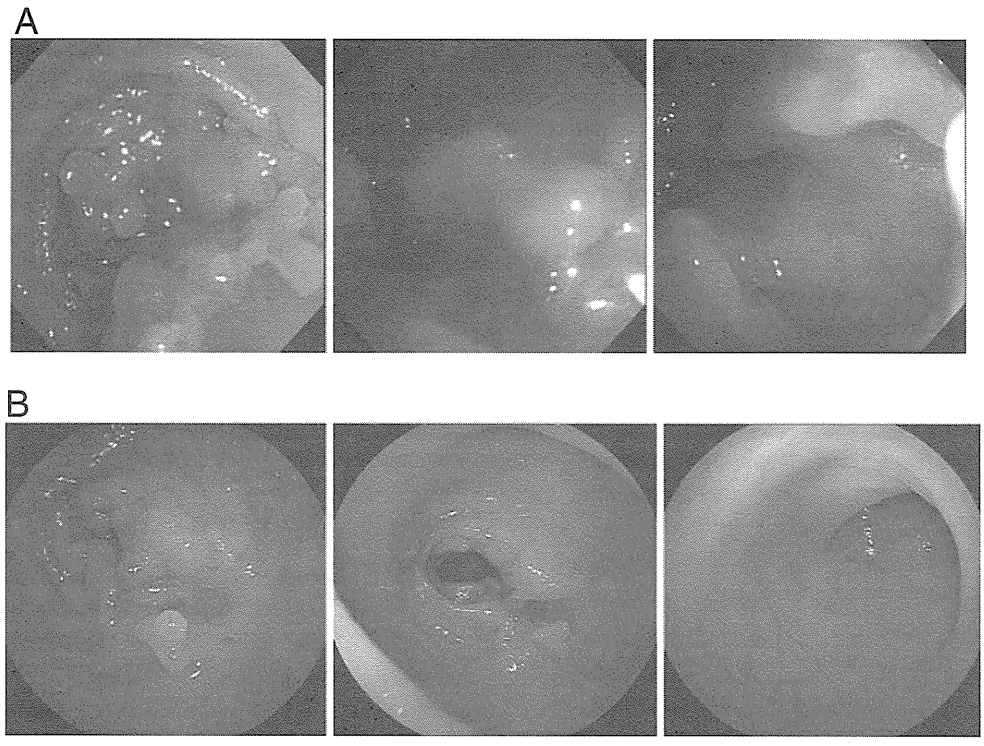

Fig. 7 Findings of colonoscopy after infliximab treatment. **a** Colonoscopy performed after the third infliximab treatment. Mild improvement was observed. Both mucosal redness and edema decreased. However, polyp-like lesions remained. At this point, the patient showed neither abdominal pain nor watery diarrhea. **b** Colonoscopy after 1-year treatment. Almost no mucosal redness or edema. A clear vascular pattern was also observed. Inflammatory polyps could still be found

reversion in T cells after co-stimulation with PHA and IL-2 before and even after infliximab therapy (Table III and Fig. 5). Reversion mosaicism has been reported in primary immunodeficiencies such as X-linked severe combined immunodeficiency [20, 21], adenosine deaminase deficiency [22], *RAG1* deficiency [23], and Wiskott–Aldrich syndrome [24]. Most of these patients reduced the frequency of severe infections and showed survival for longer periods. Our patient also had very few episodes of severe infection after expansion of IFNγ-producing peripheral blood mononuclear cells, contrary to increased susceptibility to diverse pathogens in X-EDA-ID [5, 25]. However, none of the patients with reversion mosaicism involving reverted T cells developed IBD other than X-EDA-ID. Our patient and patients with Omenn's syndrome [21, 23] developed systemic inflammatory conditions and exhibited a restricted TCR repertoire. In our patient, oligoclonal expansion of reverted T cells caused impairment of immune regulation.

According to the report by Nenci et al. in a murine model of intestinal epithelium-specific NEMO deficiency, intestinal epithelial cells exhibit increased sensitivity to TNFα-induced apoptosis and cause disruption of the epithelial barrier if mucosal immune cells have normal immune functions and produce proinflammatory cytokines [15]. They also showed that an additional TNF receptor-1 knockout ameliorated this intestinal inflammation [15]. The pathogenesis of severe colitis in the mouse model seems to be similar to that of our patient. Specifically, NEMO-deficient intestinal epithelium was damaged by TNFα produced from both T cells and macrophages in the lamina propria (shown in Fig. 3c–e, h), and anti-TNFα antibody suppressed progression of intestinal inflammation. Although reversion in peripheral blood monocytes was not confirmed after culture with GM-CSF and analysis of TNFα expression after LPS stimulation, submucosal and peripheral macrophages produced a fair amount of TNFα detectable by immunohistochemistry and flow cytometry (Figs. 3 and 4). Production of TNFα from lamina propria macrophages may be augmented by IFNγ released from reverted T cells.

In addition to the amelioration of clinical symptoms and colonic mucosal inflammation, in our patient, TNF blockade therapy restored his dry skin with thick epidermis to moderately moist skin of normal thickness. Nenci et al. described in another paper using the epidermis-specific NEMO-deficient mice that mice showed severe skin inflammation with thick epidermis and predominant infiltration of inflammatory cells and showed further that an additional knockout of TNFR1 suppressed the inflammatory condition [26]. We postulate that TNFα is also a key cytokine in the pathogenesis of inflammation in diverse epithelial tissues and that infliximab treatment suppresses the TNFα-mediated inflammatory response by inducing apoptosis of TNFα-producing cells [27]. In fact, the patient's peripheral blood TNFα-producing cells reduced along with the improvement of clinical symptoms, and this reduction provided an available marker to assess inflammatory status. Reverted cells in peripheral blood also decreased after repeated anti-TNFα antibody administrations. Unfortunately, we could not obtain consent for re-biopsy so we could not

confirm a vulnerability for apoptosis of intestinal epithelium and lamina propria after the treatment.

Since patients with X-EDA-ID were well known to have increased susceptibility to mycobacterium, and in addition, anti-TNFα monoclonal antibody indeed caused infection-related deaths in a few patients with inflammatory colitis associated with primary immunodeficiencies [28–30], the side effects of anti-TNFα monoclonal antibody treatment should be paid attention to, especially, mycobacterial infections. Before infliximab treatment, we confirmed the absence of active mycobacterial infections by culture tests for mycobacterium including atypical mycobacteria, laboratory examinations, and chest radiographs. He also has no history of Bacillus Calmette-Guérin immunization. Although the patient experienced bacterial pneumonia after his third infliximab infusion, he has not suffered from severe infections for several years. This may be because of the patient's mosaicism of mutated and reverted cells. The risks concerning severe infections and oncogenic effects [31–33] should be considered before employing infliximab for NEMO colitis.

Conclusion

Reversion of mutation in T cells contributes to the pathogenesis of mucosal immunity in NEMO-deficient patients. Moreover, treatment with anti-TNFα monoclonal antibody therapy can improve the symptoms of the disease by both preventing exposure of the mucosa to TNFα and reducing the number of T cells carrying the reverted gene. Anti-TNFα monoclonal antibody therapy provides a promising treatment for intractable NEMO colitis.

Acknowledgments We profoundly thank for Dr. Kazuko Uno of the Louis-Pasteur Medical Research Center in Japan for support of our experiments and Dr. Maiko Kai and Dr. Naoki Karasawa1 for their warm care of patients. This study was supported by a Grant-in-Aid for Scientific Research from the Ministry of Education, Culture, Sports, Science and Technology, Japan.

Conflict of Interests The authors declare no competing financial interests.

References

1. Zonana J, Elder M, Schneider L, et al. A novel X-linked disorder of immune deficiency and hypohidrotic ectodermal dysplasia is allelic to incontinentia pigmenti and due to mutations in IKK-gamma (NEMO). Am J Hum Genet. 2000;67:1555–62.
2. Döffinger R, Smahi A, Bessia C, et al. X-linked anhidrotic ectodermal dysplasia with immunodeficiency is caused by impaired NF-kappaB signaling. Nat Genet. 2001;27:277–85.
3. Jain A, Ma CA, Liu S, et al. Specific missense mutations in NEMO result in hyper-IgM syndrome with hypohydrotic ectodermal dysplasia. Nat Immunol. 2001;2:223–8.
4. Orange JS, Brodeur SR, Jain A, et al. Deficient natural killer cell cytotoxicity in patients with IKK-gamma/NEMO mutations. J Clin Invest. 2002;109:1501–9.
5. Orange JS, Jain A, Ballas ZK, et al. The presentation and natural history of immunodeficiency caused by nuclear factor kappaB essential modulator mutation. J Allergy Clin Immunol. 2004;113:725–33.
6. Pai S, Levy O, Jabara H, et al. Allogeneic transplantation successfully corrects immune defects, but not susceptibility to colitis, in a patient with nuclear factor-kappaB essential modulator deficiency. J Allergy Clin Immunol. 2008;122:1113–1118.e1111.
7. Tono C, Takahashi Y, Terui K, et al. Correction of immunodeficiency associated with NEMO mutation by umbilical cord blood transplantation using a reduced-intensity conditioning regimen. Bone Marrow Transplant. 2007;39:801–4.
8. Mancini AJ, Lawley LP, Uzel G. X-linked ectodermal dysplasia with immunodeficiency caused by NEMO mutation: early recognition and diagnosis. Arch Dermatol. 2008;144:342–6.
9. Fish J, Duerst R, Gelfand E, et al. Challenges in the use of allogeneic hematopoietic SCT for ectodermal dysplasia with immune deficiency. Bone Marrow Transplant. 2009;43:217–21.
10. Permaul P, Narla A, Hornick J, et al. Allogeneic hematopoietic stem cell transplantation for X-linked ectodermal dysplasia and immunodeficiency: case report and review of outcomes. Immunol Res. 2009;44:89–98.
11. Cheng L, Kanwar B, Tcheurekdjian H, et al. Persistent systemic inflammation and atypical enterocolitis in patients with NEMO syndrome. Clin Immunol. 2009;132:124–31.
12. Hanson E, Monaco-Shawver L, Solt L, et al. Hypomorphic nuclear factor-kappaB essential modulator mutation database and reconstitution system identifies phenotypic and immunologic diversity. J Allergy Clin Immunol. 2008;122:1169–1177.e1116.
13. Takada H, Nomura A, Ishimura M, et al. NEMO mutation as a cause of familial occurrence of Behçet's disease in female patients. Clin Genet. 2010;78:575–9.
14. Marks DJ, Miyagi K, Rahman FZ, et al. Inflammatory bowel disease in CGD reproduces the clinicopathological features of Crohn's disease. Am J Gastroenterol. 2009;104:117–24.
15. Nenci A, Becker C, Wullaert A, et al. Epithelial NEMO links innate immunity to chronic intestinal inflammation. Nature. 2007;446:557–61.
16. Nagano M, Kimura N, Ishii E, et al. Clonal expansion of alphabeta-T lymphocytes with inverted Jbeta1 bias in familial hemophagocytic lymphohistiocytosis. Blood. 1999;94:2374–82.
17. Kimura N, Toyonaga B, Yoshikai Y, et al. Sequences and repertoire of the human T cell receptor alpha and beta chain variable region genes in thymocytes. Eur J Immunol. 1987;17:375–83.
18. Nishikomori R, Akutagawa H, Maruyama K, et al. X-linked ectodermal dysplasia and immunodeficiency caused by reversion mosaicism of NEMO reveals a critical role for NEMO in human T-cell development and/or survival. Blood. 2004;103:4565–72.
19. Ogura Y, Imamura Y, Murakami Y, et al. Intracellular cytokine patterns of peripheral blood T cells as a useful indicator of activeness of Crohn's disease. Hiroshima J Med Sci. 2005;54:1–8.
20. Stephan V, Wahn V, Le Deist F, et al. Atypical X-linked severe combined immunodeficiency due to possible spontaneous reversion of the genetic defect in T cells. N Engl J Med. 1996;335:1563–7.
21. Wada T, Yasui M, Toma T, et al. Detection of T lymphocytes with a second-site mutation in skin lesions of atypical X-linked severe combined immunodeficiency mimicking Omenn syndrome. Blood. 2008;112:1872–5.
22. Hirschhorn R, Yang D, Puck J, et al. Spontaneous in vivo reversion to normal of an inherited mutation in a patient with adenosine deaminase deficiency. Nat Genet. 1996;13:290–5.
23. Wada T, Toma T, Okamoto H, et al. Oligoclonal expansion of T lymphocytes with multiple second-site mutations leads to

Omenn syndrome in a patient with RAG1-deficient severe combined immunodeficiency. Blood. 2005;106:2099–101.
24. Ariga T, Kondoh T, Yamaguchi K, et al. Spontaneous in vivo reversion of an inherited mutation in the Wiskott–Aldrich syndrome. J Immunol. 2001;166:5245–9.
25. Filipe-Santos O, Bustamante J, Haverkamp MH, et al. X-linked susceptibility to mycobacteria is caused by mutations in NEMO impairing CD40-dependent IL-12 production. J Exp Med. 2006;203:1745–59.
26. Nenci A, Huth M, Funteh A, et al. Skin lesion development in a mouse model of incontinentia pigmenti is triggered by NEMO deficiency in epidermal keratinocytes and requires TNF signaling. Hum Mol Genet. 2006;15:531–42.
27. Van den Brande J, Braat H, van den Brink G, et al. Infliximab but not etanercept induces apoptosis in lamina propria T-lymphocytes from patients with Crohn's disease. Gastroenterology. 2003;124:1774–85.
28. Nos P, Bastida G, Beltran B, et al. Crohn's disease in common variable immunodeficiency: treatment with antitumor necrosis factor alpha. Am J Gastroenterol. 2006;101:2165–6.
29. Chua I, Standish R, Lear S, et al. Anti-tumour necrosis factor-alpha therapy for severe enteropathy in patients with common variable immunodeficiency (CVID). Clin Exp Immunol. 2007;150:306–11.
30. Uzel G, Orange JS, Poliak N, et al. Complications of tumor necrosis factor-α blockade in chronic granulomatous disease-related colitis. Clin Infect Dis. 2010;51:1429–34.
31. Mackey AC, Green L, Liang LC, et al. Hepatosplenic T cell lymphoma associated with infliximab use in young patients treated for inflammatory bowel disease. J Pediatr Gastroenterol Nutr. 2007;44:265–7.
32. Mackey AC, Green L, Leptak C, et al. Hepatosplenic T cell lymphoma associated with infliximab use in young patients treated for inflammatory bowel disease: update. J Pediatr Gastroenterol Nutr. 2009;48:386–8.
33. Diak P, Siegel J, La Grenade L, et al. Tumor necrosis factor alpha blockers and malignancy in children: forty-eight cases reported to the Food and Drug Administration. Arthritis Rheum. 2010;62:2517–24.

Molecular Immunology 49 (2011) 48–55

Contents lists available at ScienceDirect

Molecular Immunology

journal homepage: www.elsevier.com/locate/molimm

Factor H gene variants in Japanese: Its relation to atypical hemolytic uremic syndrome

Saki Mukai[a], Yoshihiko Hidaka[b], Masako Hirota-Kawadobora[a], Kazuyuki Matsuda[a], Noriko Fujihara[a], Yuka Takezawa[a], Seiko Kubota[a], Kenichi Koike[b], Takayuki Honda[a,c], Kazuyoshi Yamauchi[d,*]

[a] Department of Laboratory Medicine, Shinshu University Hospital, Japan
[b] Department of Pediatrics, Shinshu University School of Medicine, Japan
[c] Department of Laboratory Medicine, Shinshu University School of Medicine, Japan
[d] Department of Medicine, Molecular Clinical Pathology, Graduate School of Comprehensive Human Sciences, University of Tsukuba, Japan

ARTICLE INFO

Article history:
Received 4 April 2011
Received in revised form 19 July 2011
Accepted 20 July 2011
Available online 24 August 2011

Keywords:
Atypical hemolytic syndrome
Factor H
Genetic analysis
Alternative complement pathway
Hemolytic assay

ABSTRACT

Mutations and polymorphisms of factor H gene (*FH1*) are known to be closely involved in the development of atypical hemolytic uremic syndrome (aHUS). Several groups have identified disease risk mutations and polymorphisms of *FH1* for the development of aHUS, and have investigated frequencies of aHUS in a number of ethnic groups. However, such studies on Japanese populations are limited. In the present study, we analyzed *FH1* in Japanese aHUS patients and healthy volunteers, and examined whether those variants impacted on a tendency for the development of aHUS in Japanese populations. Similar to previous studies, we found that a high frequency of *FH1* mutations, located in exon 23 of *FH1*, encodes short consensus repeat 20 in C-terminal end of factor H molecule in patients with aHUS (40%), but not in healthy volunteers. Interestingly, no significant differences in frequency of well-known disease risk polymorphisms for aHUS were observed between healthy volunteers and aHUS patients. Our results suggested that although *FH1* mutations relates to the development of Japanese aHUS in accordance with other ethnic studies, other factor may be required for factor H polymorphism to be a risk factor of Japanese aHUS.

1. Introduction

Hemolytic uremic syndrome (HUS) is a microvasculature disorder characterized by the triad of microangiopathic hemolytic anemia, renal failure, and thrombocytopenia, and is mainly caused by the enterocolitis with Shiga toxin-producing *Eschericia coli* of the serotype O157:H7 (Karmali et al., 1983, 1985). This form, known as typical HUS, has a good prognosis, and not often affects family members (Kaplan et al., 1998; Ault, 2000; Sánchez-Corral & Melgosa, 2010). In contrast, atypical HUS (aHUS), characterized by the absence of any infection (e.g., Shiga toxin-producing *E. coli, Shigella dysenteriae,* and *Streptococcus pneumoniae*) and its associated-diarrhea, tends to relapse and have a poor prognosis (Kaplan et al., 1998; Ault, 2000; Sánchez-Corral & Melgosa, 2010), and has been classified as either sporadic or familial (Kaplan et al., 1975). Approximately 50% of patients with aHUS have mutations in the genes encoding complement regulatory proteins [e.g., factor H, membrane cofactor protein (MCP or CD46), factor I, factor B, thrombomodulin, and C3] (Atkinson et al., 2005; Caprioli et al., 2006; Delvaeye et al., 2009). In particular, the gene coding factor H, *FH1*, is known to be the most frequently affected in the development of aHUS (Caprioli et al., 2006).

Factor H, a 150-kDa plasma glycoprotein predominantly produced in the liver, consists of 20 homologous units of about 60 amino acid residues each, known as short consensus repeats (SCRs) or the complement control protein units (Ault, 2000). Factor H plays a critical role in the regulation of the alternative complement activation pathway; i.e., this complement component is a cofactor for serine protease factor I in cleaving C3b to its inactive form (C3bi) and accelerates decay of the alternative complement pathway C3bBb convertase complex (Weiler et al., 1976; Whaley and Ruddy, 1976; Pangburn et al., 1977). Several reports demonstrated that anomalous function of factor H, attributed to the mutations in *FH1*, affects the complementary activation and the pathogenesis of aHUS (Pangburn, 2002; Sánchez-Corral et al., 2004; Ferreira and Pangburn, 2007). Actually, Saunders et al. (2006) previously demonstrated that the majority of *FH1* mutations in patients with aHUS causes either single amino acid exchange or premature translation interruption within SCR 20, a domain which contains recognition sites for cell surface ligands, and consequently the

* Corresponding author at: Department of Medicine, Molecular Clinical Pathology, Graduate School of Comprehensive Human Sciences, University of Tsukuba, 1-1-1 Tennoudai, Tsukuba, 305-8575, Japan, Tel.: +81 29 853 3456; fax: +81 29 853 3456.
E-mail address: yamauchi@md.tsukuba.ac.jp (K. Yamauchi).

0161-5890/$ – see front matter © 2011 Elsevier Ltd. All rights reserved.
doi:10.1016/j.molimm.2011.07.017

binding avidity of factor H (to C3b, heparin, or endothelial cells) is reduced.

To date, several linkage analyses have revealed that *FH1* is a candidate gene for aHUS, because its mutations or polymorphisms could be frequently detectable in aHUS patients (Caprioli et al., 2001, 2003; Richards et al., 2001; Neumann et al., 2003; Esparza-Gordillo et al., 2005). However, to our knowledge, the frequency of *FH1* mutations and polymorphisms and their relation to aHUS in Japanese subjects have not been well-defined.

We designed this study with an aim to characterize factor H and its impact on the clinical phenotype in Japanese aHUS patients. Further, we analyzed the frequency of *FH1* mutations and polymorphisms in Japanese patients with aHUS, their family members, and healthy volunteers to clarify its relevance to the pathogenesis of aHUS.

2. Materials and methods

2.1. Subjects

DNA samples were extracted from whole peripheral blood leukocytes obtained from aHUS patients [$n = 10$, 3 men and 7 women; age range 1–40 years (mean ± SE, 19 ± 5 years)], the family members (for the pedigree analysis), and healthy volunteers [$n = 15$, 3 men and 12 women; age range 26–58 years (mean ± SE, 41 ± 3 years)] using QIAamp DNA Blood Mini Kit (Qiagen, Valencia, CA) according to the manufacturer's instructions. We also used 32 healthy volunteer's sera for hemolytic assay. As described previously (Scheiring et al., 2010), aHUS was clinically defined as non-diarrheal and non-Shiga toxin HUS. This study was approved by the ethics committee of Shinshu University, Japan (approval No., 221). All subjects gave their informed consent before participation.

2.2. Serum C3

The C3 concentrations in the serum were measured by turbidimetric immunoassay method (Nittobo, Tokyo, Japan) using a BioMajesty JCA-BM 1650 (JEOL, Tokyo, Japan).

2.3. Quantification of factor H concentration

The factor H concentrations in the serum were measured by the ELISA method as described previously (Oppermann et al., 1990). Briefly, commercial polystyrene immunoplates (Nunc, Roskilde, Denmark) were coated with anti-human factor H (ANTIBODYSHOP, Gentofte, Denmark) in 50 mmol/L sodium bicarbonate, pH 10.6 (1.0 mg protein/L) for 24 h at 4 °C. Plates were washed three times with PBS containing 0.5 g/L Tween 20 (PBS-Tween) after each of the subsequent incubation steps. Unoccupied sites were blocked with the blocking buffer (NOF Corp., Tokyo, Japan) for 30 min at room temperature. The prepared calibrators and samples were then added at 100 μL/well and incubated for 2 h at room temperature. Biotinylated anti-factor H (ANTIBODYSHOP, Gentofte, Denmark) was added at 100 μL/well and incubated for 1 h at room temperature. Horseradish peroxidase-conjugated streptoavidin (Dako, Glostrup, Denmark), diluted 1000-fold with PBS-Tween, was then added at 100 μL/well and incubated for 1 h at room temperature. After final washings, the color reaction was developed with 100 μL/well of 5 g/L t-methylbenzidine dihydrochloride and hydrogen peroxide. After 30-min incubation at room temperature, the reaction was stopped by adding 50 μL of 0.4 mol/L sulfuric acid, and the absorbance at 450 nm was measured using Personal LAB (Biochem ImmunoSystems, PA). A calibration curve was generated, and the factor H concentration in serum was calculated from the curve. Each assay was carried out at lest in duplicate.

2.4. Hemolytic assay

A hemolytic assay was carried out as described previously (Pangburn, 2002) with a small modification. Briefly, sheep erythrocytes were suspended in HEPES buffer (20 mM HEPES, 7 mM $MgCl_2$, 10 mM EGTA, 144 mM NaCl, 1% BSA; pH 7.4) to give a final concentration of 5×10^4 cells/μL. One hundred microliters of the above suspension was mixed with equal volume of serial dilution series of each serum (5, 10, 20, 30, 40, and 50% serum concentration) or saline as a blank, and the mixture was immediately incubated at 37 °C for 30 min. After the mixture was centrifuged at 3500 rpm for 3 min at room temperature, absorbance at 414 nm (A_{414}) of the isolated supernatant was determined using SpectraMax PLUS384 (Molecular Devices Inc., Sunnyvale, CA). The percent hemolytic activity of each sample was determined by subtracting the A_{414} of blank, and dividing by the A_{414} of the control of total lysis (100 μL of serum, 1 μL of 5×10^6 cells/μL sheep erythrocytes suspension and 99 μL of ammonium chloride solution).

2.5. Screening for factor H antibody

The factor H antibodies in the serum were identified by the ELISA method as described previously (Dragon-Durey et al., 2005) with a small modification. Briefly, commercial polystyrene immunoplates were coated with human factor H (Calbiochem, Meudon, France) in PBS (0.3 μg/well) for 24 h at 4 °C. Plates were washed three times after each of the subsequent incubation steps, and blocked unoccupied sites with PBS containing 10 g/L BSA for 1 h at room temperature. The samples were added at at 100 μL/well diluted 1:10 for 1 h at room temperature. Horseradish peroxidase-conjugated goat anti-human IgG solution (Denka-Seiken, Tokyo, Japan) was then added at 100 μL/well and incubated for 1 h at room temperature. After final washings, the color reaction was developed using t-methylbenzidine dihydrochloride and hydrogen peroxide. After 30-min incubation at room temperature, the reaction was stopped by adding 100 μL of 0.3 mol/L sulfuric acid, and the absorbance at 450 nm was measured using Personal LAB. Absorbance above the mean + 2SD of those determined by making measurements of 37 healthy volunteers' sera was considered as positive.

2.6. Screening of FH1 mutations and polymorphisms

FH1 exons were identically amplified by conventional PCR method. The primers used in present study are listed in Table 1. We designed 3 specific primer sets which amplify exons 22 and 23, including C3645T mutation (Ser1191Leu in SCR20) and G3717A mutation (Arg1215Gln in SCR20), and 6 specific primer sets used for recognizing polymorphisms [(C-257T in promoter region, C994A in exon 7 (Ala307Ala in SCR5), G1492A in exon 9 (Ala473Ala in SCR8), A2089G in exon 14 (Gln672Gln in SCR11), G2881T in exon 19 (Glu936Asp in SCR16), and G3364A in exon 20 (Thr1097Thr in SCR18)] according to previous study (Caprioli et al., 2003). PCR was performed on a Gene Amp PCR system 9700 (Applied Biosystems, Foster City, CA). After the purification of PCR products, direct DNA sequencing was performed using a BigDye™ Terminator Cycle Sequencing Ready Reaction Kit and an ABI Prism 3100 Genetic Analyzer (both from Applied Biosystems).

2.7. Statistical methods

All experiments were performed at least three times. Data are presented as mean ± 2SD. Statistical analysis was performed by non-paired t test and chi-square test depending on the data set concerned. A p value of less than 0.05 was accepted as statistically significant.

Table 1
Primers set for factor H gene (FH1) screening.

Region	SCR	Foward	Reverse
Promoter	–	5′-CAAGCACTGCATTCTTGGCA-3′	5′-GCTAGGGAAATTCTCCGTTG-3′
exon 7	SCR 5	5′-TTTAACGGATACTTATTTCTGCATTATCC-3′	5′-TTCAGAATTAAGAAATGGGTCAAGATATG-3′
exon 9	SCR 8	5′-ATAGATATTGAATGGGTTTATTTCTGAA-3′	5′-GTTGAGCTGACCATCCATCTTTC-3′
exon 14	SCR 11	5′-TATATTGTAAAACAGACAATTTAACC-3′	5′-ATACAAAATACAAAAGTTTTGACAAG-3′
exon 19	SCR 16	5′-GATGTCATAGTAGCTCCTGTATTGTTTATTT-3′	5′-CCACTTACACTTTGAATGAAGAATATTTATC-3′
exon 20	SCR 18	5′-CACTTCTTTTTTTTCTATTCAGACACC-3′	5′-AGAATTGAATTTTAAGCACCATCAG-3′
exon 22	SCR 19	5′-TGAAATATCAGACTCATCACAGA-3′	5′-ATACAGTGCTGTGTTTGCG-3′
exon 23	SCR20[a]	5′-GTTCTGAATAAAGGTGTGCAC-3′	5′-GCCAAACAGAAGCTTTATTC-3′
exon 23	SCR20[b]	5′-CCCCGTTACACACAAATTCAA-3′	5′-CTACATAGTTGGTTTGGAT-3′

[a] Upstream region of exon 23.
[b] Downstream region of exon 23.

3. Results

3.1. Clinical features of patients with aHUS

Clinical features and genetic findings of *FH1* of 10 patients with aHUS were summarized in Tables 2 and 3, respectively.

Patient 1 (A-6). We analyzed for factor H status using patient's serum, obtained after 1-yr from the episode. Serum factor H level was also significantly decreased (75% of healthy volunteer's serum, $p < 0.01$). The heterozygous G3717A mutation, and heterozygous polymorphisms of C-257T, A2089G, G2881T, and G1492A were found in FH1. Anti-factor H antibody was not detected. Other complement regulatory factors were normal (i.e., factor I level was 14.5 mg/dl, and expression of MCP on lymphocytes was not decreased). The ADAMTS13 activity was normal.

Patient 2 (B-11). We analyzed for factor H status using patient's serum, obtained after 3-yrs from the first episode. Factor H level was slightly increased (114% of healthy volunteer's serum, $p < 0.01$). The heterozygous G3717A mutation, and five heterozygous disease risk polymorphisms (C-257T, A2089G, G2881T, C994A, G1492A,

Table 2
Clinical features of aHUS patients.

Case (Pedigree No)	Age	Gender	Onset age	Clinical findings and evolutions
1 (A-6)	1 yr	F	4 mo	Renal insufficiency and hypocomplementemia. Under treatment (plasmapheresis and FFP administration).
2 (B-11)	34 yr	M	31 yr	Renal insufficiency, hemolytic anemia, biliruminemia, hypocomplementemia, and thrombocytopenia. Under treatment (Chronic hemodialysis and plasmapheresis).
3 (B-12)	38 yr	F	31 yr	Hypocomplementemia. Under treatment (Chronic hemodialysis).
4 (C-6)	29 yr	F	6 mo	Hemolytic anemia, and thrombocytopenia. Recurrence of aHUS after pregnancy and partum. Remission after PSL administration and steroid pulse therapy.
5 (D-3)	17 yr	F	13 yr	Renal insufficiency, hemolytic anemia, bilirubinemia, and thrombocytopenia. Remission after continuous hemodialysis.
6	4 yr	F	n.c.	Renal insufficiency, hemolytic anemia, and thrombocytopenia. Under treatment (plasmapheresis).
7	8 yr	M	4 yr	Renal insufficiency, hemolytic anemia, bilirubinemia, thrombocytopenia and hypocomplementemia. Recurrence of aHUS after infection of influenzavirus B. Under supportive treatment.
8	40 yr	M	40 yr	Renal insufficiency, and hemolytic anemia. Under treatment (hemodialysis, plasmapheresis, PSL administration, and steroid pulse therapy).
9	7 yr	F	7 mo	Severe thrombocytopenia. Recurrence. Before treatment.
10	9 yr	F	n.c.	Renal insufficiency, hemolytic anemia, thrombocytopenia, and hypocomplementemia. Before treatment.

FFP, fresh frozen plasama; PSL, prednisolone; n.c., not clear.

Table 3
Factor H status in Japanese Ahus.

Case (pedigree no.)	Polymorphisms						Mutation	Serum factor H levels	Hemolytic activity[b]	Anti-factor H antibody
	C-257T	C994A	G1492A	A2089G	G2881T	G3364A	G3717A	(relative to normal value %)[a]		
1 (A-6)	CT	CC	GA	AG	GT	GG	AG	75*	+	–
2 (B-11)	CT	CA	GA	AG	GT	GG	AG	114*	–	–
3 (B-12)	CC	CA	GA	AA	GG	GG	AG	131*	+	–
4 (C-6)	CC	CC	AA	AA	GG	GG	GG	74*	–	–
5 (D-3)	CC	CC	AA	AA	GG	GG	GG	n.t.	–	–
6	CC	CC	AA	AA	GG	GG	GG	62*	+	+
7	CT	CA	n.d.	AA	GG	GA	GG	108	+	–
8	TT	CC	GA	GG	TT	GG	GG	143*	+	–
9	TT	CC	GG	GG	TT	GA	GG	125*	–	–
10	TT	CC	GG	GG	TT	GA	GG	80*	–	+

[a] Serum factor H levels were expressed as the relative to normal value (1388 ± 547 mg/L), determined by making measurements of healthy volunteers' sera.
[b] The percent hemolytic activity of each patient's serum was compared with those of normal value, determined by making measurements of 32 healthy volunteers' sera as described in Section 2. The subjects with a significantly high level of hemolytic activity were expressed as "positive". n.d., not determined. n.t., not tested.
* $p < 0.01$ vs normal value.

and G3364A) were found in FH1. Anti-factor H antibody was not detected.

Patient 3 (B-12). We analyzed for factor H status using patient's serum, obtained after 7-yrs from the first episode. Factor H level was significantly increased (131% of healthy volunteer's serum, $p < 0.01$). The heterozygous G3717A mutation and two heterozygous disease risk polymorphisms (C994A and G1492A) were found in FH1. In addition, we found the novel silent mutation [C3013T (His980His)] in exon 18. Anti-factor H antibody was not detected.

Patient 4 (C-6). We analyzed for factor H status using patient's serum, obtained after 2-months from the first episode. Factor H level was significantly decreased (74% of healthy volunteer's serum, $p < 0.01$); however, we found neither mutation nor disease risk polymorphism of aHUS in FH1. Anti-factor H antibody was not detected.

Patient 5 (D-3). We analyzed for factor H status using patient's serum, obtained after 4-yrs from the episode. Factor H level was significantly decreased (64% of healthy volunteer's serum, $p < 0.01$); however, we confirmed that this patient had neither mutation nor disease risk polymorphism of aHUS in FH1. Anti-factor H antibody was not detected.

Patient 6. We analyzed for factor H status using patient's serum, obtained after 6-months from the episode. Serum factor H level was significantly decreased (62% of healthy volunteer's serum, $p < 0.01$). We found neither mutation nor disease risk polymorphism of aHUS in FH1, however, we could detect anti-factor H antibody.

Patient 7. We analyzed for factor H status using patient's serum, obtained on admission. Although serum factor H level was normal, we found heterozygous polymorphisms of A C-257T, C994A, and G3364A in FH1. Conservative therapy slowly improved his clinical condition and increased serum factor H level (138% of healthy volunteer's serum, $p < 0.01$). Anti-factor H antibody was not detected.

Patient 8. We analyzed for factor H status using patient's serum, obtained on admission. Serum factor H level was significantly increased (145% of healthy volunteer's serum, $p < 0.01$). The homozygous polymorphisms of C-257T, A2089G, G2881T, and the heterozygous G1492A polymorphism were found in FH1. Furthermore, we found C3645T (Ser1191Leu) mutation in exon 23 (data not shown). Anti-factor H antibody was not detected.

Patient 9. We analyzed for factor H status using patient's serum, obtained on admission. Serum factor H level was significantly increased (125% of healthy volunteer's serum, $p < 0.01$). The homozygous polymorphisms of C-257T, A2089G, G2881T were found in FH1. Anti-factor H antibody was not detected.

Patient 10. We analyzed for factor H status using patient's serum, obtained on admission. Serum factor H level was also significantly decreased (80% of healthy volunteer's serum, $p < 0.01$). We found the homozygous polymorphisms of C-257T, A2089G, G2881T were found in FH1, and detected anti-factor H antibody.

3.2. Pedigree analysis

Further, to clarify the impact of factor H genetic status on the development of aHUS, we analyzed *FH1* mutations and polymorphisms in family members of above 5 patients, and investigated their clinical histories.

3.2.1. Family A

The pedigree of family A is shown in Fig. 1A. We identified that a G3717A mutation of the proband [A-6 (Patient 1)] was inherited from a paternal allele (A-4), and that all three polymorphisms (C-257T, A2089G, G1492A) was from a maternal allele (A-5). The allele sequences of the paternal grandfather (A-1), who died of thrombocytopenic purpura (TTP), were able to be determined from those of the paternal grandmother (A-2) and a paternal uncle (A-3). Taken together, a G3717A mutation of the proband was proved to have originated from paternal grandfather.

3.2.2. Family B

The pedigree of family B is shown in Fig. 1B. Two probands [B-11 (Patient 2) and B-12 (Patient 3)] are cousins to each other, and their maternal grandfather (B-1) had died of juvenile renal insufficiency at age 42 yrs. We identified a G3717A mutation in both probands (B-11 and B-12) that was inherited from each mother (B-9 and B-10), respectively, by taking into consideration of pedigree analysis results and their clinical histories, and estimated that the mutation containing the allele originated from B-1. Further, we estimated that the three polymorphisms (C-257T, A2089G, and G2881T) of their mother's eldest sister (B-3), who has intermittent episodes of recurrent renal insufficiency, were inherited from the other allele of B-1. The *FH1* in B-5 was not able to be determined. B-4, B-6, B-7, and B-8 had already died of other causes.

3.2.3. Family C

The pedigree of family C is shown in Fig. 1C. Similar to the proband [C-6 (Patient 4)], her elder brother (C-4, 33-yr-old) and nephew (C-8, 7-yr-old) had been diagnosed as aHUS. However, their *FH1* were not able to be analyzed in present study. Her mother (C-2) had three heterozygous polymorphisms (C-257T, A2089G, and G2881T), but had no episodes of HUS. Her elder sister (C-3) inherited these three polymorphisms without episodes of HUS; whereas, the proband (C-6) did not inherit any of those polymorphisms.

3.2.4. Family D

The pedigree of family D is shown in Fig. 1D. The proband's mother (D-2) without episodes of HUS had three heterozygous polymorphisms (C-257T, A2089G, and G2881T). The proband [D-3 (Patient 5)] did not inherit any polymorphisms from her mother.

3.3. Biochemical characterization of factor H in aHUS patients

To characterize factor H in aHUS patients' sera biochemically, we performed immunoblot analysis using specific antibody against factor H. We detected the main band with a molecular weight of 150 kDa, corresponding to factor H protein, and the faint band with a molecular weight of 43 kDa, corresponding to factor H-like-protein 1 (Zipfel & Skerka, 1999; Ault, 2000), in all subjects. As well as in normal control, no extra band was observed in all subjects (data not shown).

Further, to investigate the function of factor H, we carried out the hemolytic assay using sheep erythrocytes as described in Section 2. The reference value of the percent hemolytic activity was determined by making measurements of 32 healthy volunteers' sera. The individual differences in the percent hemolytic activities were minimum at 5% serum concentration among serum dilution series (CV, 14%); thus, we defined the mean hemolytic activity at 5% serum concentration as a provisional reference value (mean $\pm$ 2SD, $12 \pm 3\%$). We then compared the percent hemolytic activity of each patient's serum with the reference value. Five of 10 aHUS patients (Patients 1, 3, 6, 7, and 8) presented with a significantly high level of hemolytic activity (Fig. 2). When we added recombinant factor H, with a final concentration of 1.1 mg/dl, significantly suppressed the accelerated hemolytic activities of 5 all patients (data not shown). Three of these 5 patients (Patients 1, 3, and 8) had mutation in exon 23 that encodes for SCR 20. Patient 4 had neither mutation nor polymorphism, despite having a low level of serum factor H. Patient 5 had three heterozygous polymorphisms, but no mutations, with a normal level of serum factor H. On the other hand, although Patient 2 had a mutation in exon 23, his hemolytic activity exhibited the normal level. Overall, no correlation between the hemolytic activity

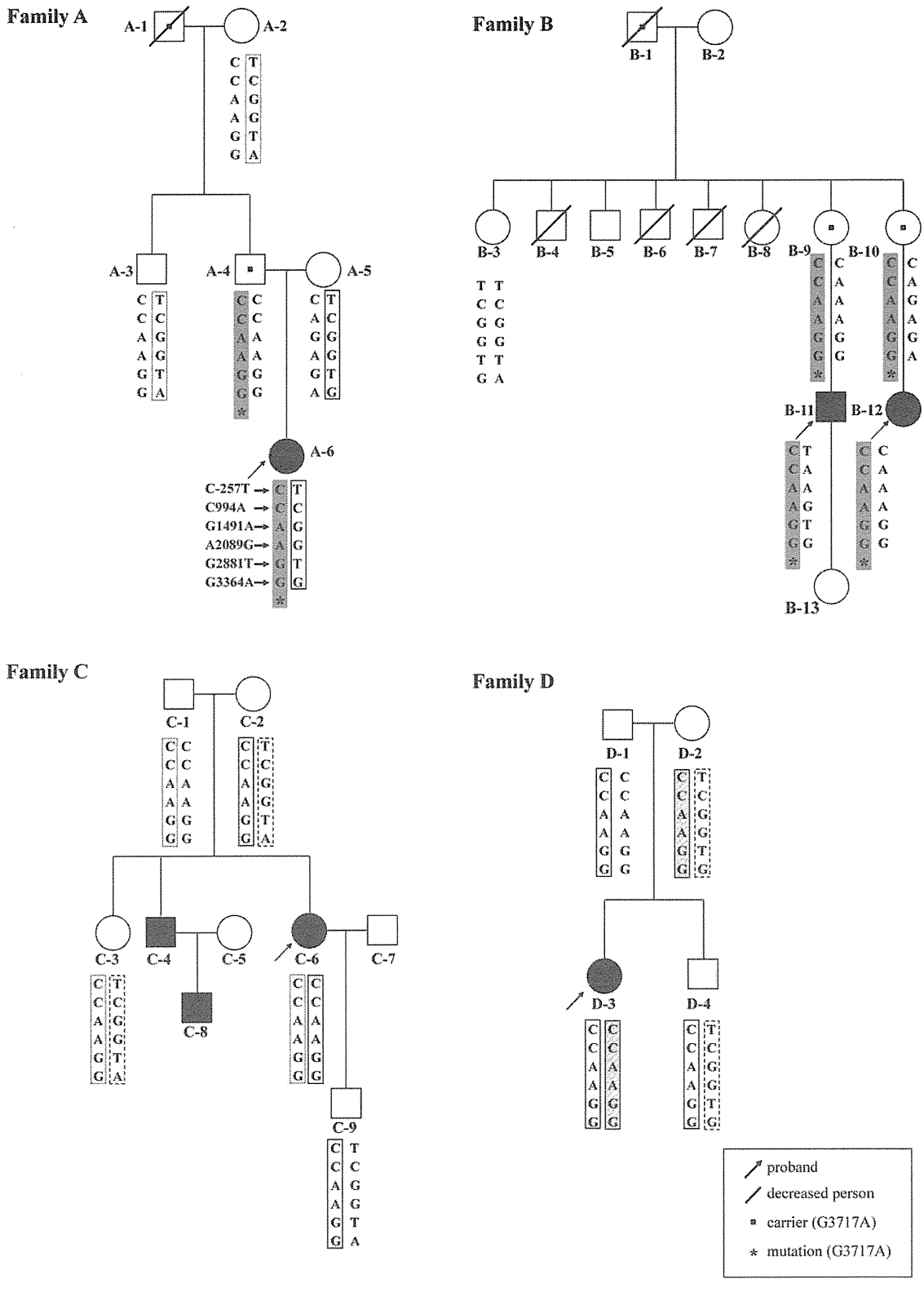

Fig. 1. Pedigree of families A, B, C, and D. We analyzed the data for mutations and polymorphisms in *FH1* as described in Section 2. Arrows, probands; squares, men; circles, women; slashes, deceased; black asterisk, G3717A mutation; central black squares, carriers of G3717A mutation.

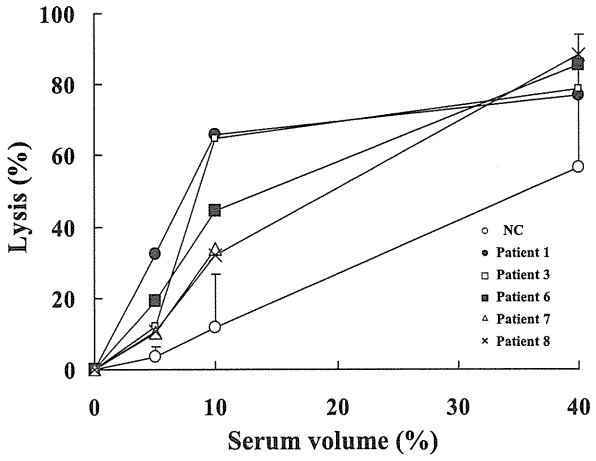

Fig. 2. Hemolytic assay. Lysis of sheep erythrocytes by serum obtained from aHUS patients [solid circles, Patient 1 (with G3717A); open square, Patient 3 (with G3717A), solid square, Patient 6 (without mutation); triangles, Patient 7 (without mutation); crosses, Patient 8 (with C3645T mutation)]. The percent hemolytic activity of 32 healthy volunteers' sera shown (open circles) are mean + 2SD. (b) Inhibition of the lysis by factor H. We added recombinant factor H to each patients' serum to give final factor H concentrations of 1.1 mg/dl. Lysis (%) [with (shaded bars) or without (open bars) recombinant factor H] was determined at 5% serum concentration after a 30-min incubation. Data are expressed as mean ± 2SD from duplicate determinations in each of three separate experiments. *: $P < 0.05$ and **: $P < 0.01$ compared with the lysis (%) of each patient serum without recombinant factor H.

and factor H level was observed. The specificity of a hemolytic assay for the detection of aHUS was insufficient (50%), but the sensitivity was 100%.

3.4. Allele frequencies of factor H gene mutations and polymorphisms

To evaluate the effects of mutations and polymorphisms in *FH1* on the development of aHUS in Japanese, we compared the frequency of *FH1* mutations and polymorphisms in aHUS patients with that in healthy volunteers. As summarized in Table 3, no significant differences in the frequencies of all 6 disease risk polymorphisms, identified previously (Caprioli et al., 2003), were observed between aHUS patients and healthy volunteers. However, the mutations in exon 23 of FH1 (A3717G or C3645T) were highly frequent, but not statistically significant, detected in aHUS patients (40%).

4. Discussion

In the present study, we identified *FH1* mutation in 4 of 10 aHUS patients. All of those mutations, located in exon 23 of *FH1*, encode SCR 20 (3 Arg1215Gln mutations and 1 Ser1191Leu mutation). Previous studies demonstrated that the majority of the mutations associated with aHUS are clustered at the SCR 20 in C-terminal end of factor H molecule, which plays a critical role as both C3 (C3d fragment)- and heparin-binding sites (Blackmore et al., 1998; Ault, 2000; Caprioli et al., 2001). Three of these patients presented with a significantly high level of hemolytic activity. The serum factor H level of Patient 1 was only modestly decreased, and those of Patient 3 and Patient 8 were increased rather than decreased. These findings supported the notion that those mutations in SCR 20 may impair the function of factor H in the alternative complement cascade on cell surface (Rodríguez de Córdoba et al., 2004) and subsequently cause the development of aHUS.

Hemolytic assays using sheep erythrocytes have been thought to be useful for the detection of factor H-related complement regulatory defects and molecular diagnosis of factor H-related aHUS (Sánchez-Corral et al., 2004). Notably, however, we revealed several discrepancies between the existence of the *FH1* mutation and the results of hemolytic assays in three cases. First, two patients (Patient 6 and Patient 7) presented with significantly high levels of hemolytic activity, even though they had no mutations in the well-known hot spot of *FH1*. In case of Patient 6, autoantibody may possibly interfere with the reaction on the quantification of serum factor H as described previously (Dragon-Durey et al., 2005; Józsi et al., 2007). It differed from Patient 6 with a low level of serum factor H, interestingly, Patient 7 presented with a normal level of serum factor H. Although we could not exclude the influence of some medical treatments (especially, plasma infusion) on specimens, used for the quantification of serum factor H, the addition of recombinant factor H markedly improved hemolytic activities of both patients, providing compelling evidence that these patients have factor H-related complement regulatory defects, attributed to some variants in other region of *FH1*, which were not analyzed in present study. In general, mutations are categorized into the type I mutations with a significant reduction of the coded proteins and the type II mutations with an anomalous activity of the coded proteins. Our findings suggested that Patient 7 possibly carry some type II mutations. Second, despite the presence of Arg1215Gln mutation in SCR 20, one patient (Patient 2) presented with a normal or slightly high level of hemolytic activity. While the reduction of serum C3 in this patient arguably indicated that a complementary pathway was excessively activated, serum factor H level in this patient was slightly increased; thus, one possible reason for this discrepancy is that the dysfunction of innate factor H may cause up-regulation of factor H production, even an immature one. Further studies will be necessary to clarify the reason for these discrepancies.

We showed that 4 of 10 aHUS patients presented with normal levels of hemolytic activity and without any mutations in SCR 20. We could detect anti-factor H antibody in serum of Patient 10; therefore, autoantibody may possibly interfere with the reaction on the quantification of serum factor H. Although the pathogenesis of Patient 9 was difficult to interpret only by the results of the present study, those of other 2 patients (Patient 4 and 5) could be supposed to be caused by the reduction of serum factor H level. This finding suggests the possibility that the production of mature factor H protein might be impaired by some *FH1* abnormality, such as aberrations in alternative splicing, based on the mutation in the region of *FH1* introns. Atkinson et al. (2005) previously demonstrated that approximately 50% of patients with aHUS have a mutation in one of three genes, encoding factor H (20–30%), MCP (10–20%), or factor I (10–20%). Hence, we also should take account of the aberrations in other complementary regulatory factors, and so it will be necessary to do additional experiments.

The results of pedigree analysis for family A and B also supported the notion that a mutation in the region of *FH1*, encoding SCR 20 of factor H, could be one of potent causative risk factors for the development of aHUS, although the proband's father (A-4) in family A and both probands' mother (B-9 and B-10) in family B had no episodes, even though they had this mutation. In contrast, we could not find any remarkable features in *FH1* in the pedigree analysis for family C and D. However, as described above, we cannot completely deny the factor H dysfunction, derived from some aberration of *FH1*. The marked reduction of serum factor H level in Patient 4 (C-6) leads to the above conclusions. In particular, despite having no episodes, her son (C-9) also presented with marked reduction of serum factor H level, suggesting that he might inherit some aberration of *FH1* (possibly some type I mutations in *FH1*) from his mother [Patient 4 (C-6)], but not any effects of autoantibodies. Furthermore, the clinical differences between Patient 4 (C-6) and her son (C-9) suggested that aberrations of *FH1* may not be an independent risk factor for aHUS. As described previously (Rodríguez de Córdoba et al., 2004; Noris & Remuzzi, 2009), other triggers may promote the development of aHUS. In fact, Patient 4 (C-6) had relapsed after pregnancy

and partum. She also presented with an upper respiratory tract inflammation at relapse. These clinical findings were of importance to clarify the detailed pathogenic mechanism of aHUS.

Caprioli et al. (2003) and Neumann et al. (2003) previously reported that several polymorphisms in *FH1*, so-called disease risk polymorphisms, are frequently detected in aHUS patients more than healthy volunteers in Caucasians and German registries, respectively. We examined the allele frequencies of those disease risk polymorphisms in Japanese populations (see Section 2). Of interest, no significant difference in frequency of disease risk polymorphisms was observed between healthy volunteers and aHUS patients in Japanese groups, although the present study includes a limitation in that the results were obtained from small mass analyses. Previous studies (Blom et al., 2008; Martínez-Barricarte et al., 2008) have demonstrated racial differences in the relevance of a polymorphism in the C4b-binding protein, a regulator of the classical pathway of complementary activation, in the development of aHUS. Similarly, our findings suggest that ethnicity may affect the linkage between carrying the disease risk polymorphism in factor H and the development of aHUS.

In conclusion, our results are consistent with those of prior studies for other populations showing that FH1 mutations relates to the development of Japanese aHUS; whereas, of interest, the well-known disease risk polymorphisms of FH1 have been detected in most healthy Japanese. This finding suggested that some 'second hit' (e.g., a mutation in FH1, unknown polymorphisms in FH1, or variants of other complement regulatory factors) may be required for factor H polymorphism to be a risk factor of Japanese aHUS.

Competing interests

None.

Ethical approval

The study was approved by the ethics committee of Shinsyu University (approval No., 221).

Guarantor

KY.

Contributorship

KY has designed and supervised the project, SM, YH, MH, and KM have carried out the project, SM has written the first draft of the manuscript, NF, YK and SK have been the laboratory methods consultants, and KK and TH commented on drafts of the manuscript.

Acknowledgements

We gratefully acknowledge Dr Toshiko Kumagai and Dr Mitsutoshi Sugano (Department of Laboratory Medicine, Shinshu University Hospital) for their advices and encouragement. This work was partially supported by Nagano Society for the Promotion of Science.

References

Atkinson, J.P., Liszewski, M.K., Richards, A., Kavanagh, D., Moulton, E.A., 2005. Hemolytic uremic syndrome: an example of insufficient complement regulation on self-tissue. Ann. N. Y. Acad. Sci. 1056, 144–152.

Ault, B.H., 2000. Factor H and the pathogenesis of renal diseases. Pediatr. Nephrol. 14, 1045–1053.

Blackmore, T.K., Hellwage, J., Sadlon, T.A., Higgs, N., Zipfel, P.F., Ward, H.M., Gordon, D.L., 1998. Identification of the second heparin-binding domain in human complement factor H. J. Immunol. 160, 3342–3348.

Blom, A.M., Bergström, F., Edey, M., Diaz-Torres, M., Kavanagh, D., Lampe, A., Goodship, J.A., Strain, L., Moghal, N., McHugh, M., Inward, C., Tomson, C., Frémeaux-Bacchi, V., Villoutreix, B.O., Goodship, T.H.J., 2008. A novel non-synonymous polymorphism (p.Arg240His) in C4b-binding protein is associated with atypical hemolytic uremic syndrome and leads to impaired alternative pathway cofactor activity. J. Immunol. 180, 6385–6391.

Caprioli, J., Bettinaglio, P., Zipfel, P.F., Amadei, B., Daina, E., Gamba, S., Skerka, C., Marziliano, N., Remuzzi, G., Noris, M., 2001. The molecular basis of familial hemolytic uremic syndrome: mutation analysis of factor H gene reveals a hot spot in short consensus repeat 20. J. Am. Soc. Nephrol. 12, 297–307.

Caprioli, J., Castelletti, F., Bucchioni, S., Bettinaglio, P., Bresin, E., Pianetti, G., Gamba, S., Brioschi, S., Daina, E., Remuzzi, G., Noris, M., 2003. Complement factor H mutations and gene polymorphisms in haemolytic uraemic syndrome: the C-257T, the A2089G and the G2881T polymorphisms are strongly associated with the disease. Hum. Mol. Genet. 12, 3385–3395.

Caprioli, J., Noris, M., Brioschi, S., Pianetti, G., Castelletti, F., Bettinaglio, P., Mele, C., Bresin, E., Cassis, L., Gamba, S., Porrati, F., Bucchioni, S., Monteferrante, G., Fang, C.J., Liszewski, M.K., Kavanagh, D., Atkinson, J.P., Remuzzi, G., 2006. For the international registry of recurrent and familial HUS/TTP Genetics of HUS: the impact of MCP CFH, and IF mutations on clinical presentation, response to treatment, and outcome. Blood 108, 1267–1279.

Delvaeye, M., Noris, M., De Vriese, A., Esmon, C.T., Esmon, N.L., Ferrell, G., Del-Favero, J., Plaisance, S., Claes, B., Lambrechts, D., Zoja, C., Remuzzi, G., Conway, E.M., 2009. Thrombomodulin mutations in atypical hemolytic-uremic syndrome. N. Engl. J. Med. 361, 345–357.

Dragon-Durey, M.A., Loirat, C., Cloarec, S., Macher, M.A., Blouin, J., Nivet, H., Weiss, L., Fridman, W.H., Frémeaux-Bacchi, V., 2005. Anti-factor H antibodies associated with atypical hemolytic uremic syndrome. J. Am. Soc. Nephrol. 16, 555–563.

Esparza-Gordillo, J., Goicoechea de Jorge, E., Buil, A., Carreras-Berges, L., López-Trascasa, M., Sánchez-Corral, P., Rodríguez de Córdoba, S., 2005. Predisposition to atypical hemolytic uremic syndrome involves the concurrence of different susceptibility alleles in the regulators of complement activation gene cluster in 1q32. Hum. Mol. Genet. 14, 703–712.

Ferreira, V.P., Pangburn, M.K., 2007. Factor H mediated cell surface protection from complement is critical for the survival of PNH erythrocytes. Blood 110, 2190–2192.

Józsi, M., Strobel, S., Dahse, H.M., Liu, W.S., Hoyer, P.F., Oppermann, M., Skerka, C., Zipfel, P.F., 2007. Anti factor H autoantibodies block C-terminal recognition function of factor H in hemolytic uremic syndrome. Blood 110, 1516–1518.

Karmali, M.A., Petric, M., Lim, C., Fleming, P.C., Steele, B.T., 1983. *Escherichia coli* cytotoxin, haemolytic-uraemic syndrome, and haemorrhagic colitis. Lancet 322, 1299–1300.

Karmali, M.A., Petric, M., Lim, C., Fleming, P.C., Arbus, G.S., Lior, H., 1985. The association between idiopathic hemolytic uremic syndrome and infection by verotoxin-producing *Escherichia coli*. J. Infect. Dis. 151, 775–782.

Kaplan, B.S., Chesney, R.W., Drummond, K.N., 1975. Hemolytic uremic syndrome in families. N. Engl. J. Med. 292, 1090–1093.

Kaplan, B.S., Meyers, K.E., Schulman, S.L., 1998. The pathogenesis and treatment of hemolytic uremic syndrome. J. Am. Soc. Nephrol. 9, 1126–1133.

Martínez-Barricarte, R., Goicoechea de Jorge, E., Montes, T., Layana, A.G., Rodríguez de Córdoba, S., 2008. Lack of association between polymorphisms in C4b-binding protein and atypical haemolytic uraemic syndrome in the Spanish population. Clin. Exp. Immunol. 155, 59–64.

Neumann, H.P., Salzmann, M., Bohnert-Iwan, B., Mannuelian, T., Skerka, C., Lenk, D., Bender, B.U., Cybulla, M., Riegler, P., Königsrainer, A., Neyer, U., Bock, A., Widmer, U., Male, D.A., Franke, G., Zipfel, P.F., 2003. Haemolytic uraemic syndrome and mutations of the factor H gene: a registry-based study of German speaking countries. J. Med. Genet. 40, 676–681.

Noris, M., Remuzzi, G., 2009. Atypical hemolytic-uremic syndrome. N. Engl. J. Med. 361, 1676–1687.

Oppermann, M., Baumgarten, H., Brandt, E., Gottsleben, W., Kurts, C., Götze, O., 1990. Quantitation of components of the alternative pathway of complement (APC) by enzyme-linked immunosorbent assays. J. Immunol. Methods 133, 181–190.

Pangburn, M.K., Schreiber, R.D., Müller-Eberhard, H.J., 1977. Human complement C3b inactivator: isolation, characterization, and demonstration of an absolute requirement for the serum protein β1H for cleavage of C3b and C4b in solution. J. Exp. Med. 146, 257–270.

Pangburn, M.K., 2002. Cutting edge: localization of the host recognition functions of complement factor H at the carboxyl-terminal: implications for hemolytic uremic syndrome. J. Immunol. 169, 4702–4706.

Richards, A., Buddles, M.R., Donne, R.L., Kaplan, B.S., Kirk, E., Venning, M.C., Tielemans, C.L., Goodship, J.A., Goodship, T.H.J., 2001. Factor H mutations in hemolytic uremic syndrome cluster in exons 18–20, a domain important for host cell recognition. Am. J. Hum. Genet. 68, 485–490.

Rodríguez de Córdoba, S., Esparza-Gordillo, J., Goicoechea de Jorge, E., Lopez-Trascasa, M., Sánchez-Corral, P., 2004. The human complement factor H: functional roles, genetic variations and disease associations. Mol. Immunol. 41, 355–367.

Sánchez-Corral, P., González-Rubio, C., Rodríguez de Córdoba, S., López-Trascasa, M., 2004. Functional analysis in serum from atypical hemolytic uremic syndrome patients reveals impaired protection of host cells associated with mutations in factor H. Mol. Immunol. 41, 81–84.

Sánchez-Corral, P., Melgosa, M., 2010. Advances in understanding the aetiology of atypical haemolytic uraemic syndrome. Br. J. Haematol. 150, 529–542.

Saunders, R.E., Goodship, T.H.J., Zipfel, P.F., Perkins, S.J., 2006. An interactive web database of factor H-associated hemolytic uremic syndrome mutations: insights into the structural consequences of disease-associated mutations. Hum. Mutat. 27, 21–30.
Scheiring, J., Rosales, A., Zimmerhackl, L.B., 2010. Clinical practice Today's understanding of the haemolytic uraemic syndrome. Eur. J. Pediatr. 169, 7–13.
Weiler, J.M., Daha, M.R., Austen, K.F., Fearon, D.T., 1976. Control of the amplification convertase of complement by the plasma protein β1H· Proc. Natl. Acad. Sci. U. S. A. 73, 3268–3272.
Whaley, K., Ruddy, S., 1976. Modulation of the alternative complement pathway by β1H globulin. J. Exp. Med. 144, 1147–1163.
Zipfel, P.F., Skerka, C., 1999. FHL-1/reconectin: a human complement and immune regulator with cell-adhesive function. Immunol. Today 20, 135–140.

Aurora kinase A-specific T-cell receptor gene transfer redirects T lymphocytes to display effective antileukemia reactivity

*Kozo Nagai,[1] *Toshiki Ochi,[1] Hiroshi Fujiwara,[1,2] Jun An,[1] Toshiaki Shirakata,[1] Junichi Mineno,[3] Kiyotaka Kuzushima,[4] Hiroshi Shiku,[5] J. Joseph Melenhorst,[6] Emma Gostick,[7] David A. Price,[7] Eiichi Ishii,[8] and Masaki Yasukawa[1,2]

[1]Department of Bioregulatory Medicine, Ehime University Graduate School of Medicine, Ehime, Japan; [2]Department of Cell Growth and Cancer Regulation, Ehime University Proteomedicine Research Center, Ehime, Japan; [3]Takara Bio Inc Center for Cell and Gene Therapy, Shiga, Japan; [4]Division of Immunology, Aichi Cancer Center, Aichi, Japan; [5]Department of Cancer Vaccine and Immuno-Gene Therapy, Mie University Graduate School of Medicine, Mie, Japan; [6]Hematology Branch, National Heart, Lung, and Blood Institute, National Institutes of Health, Bethesda, MD; [7]Department of Infection, Immunity and Biochemistry, Cardiff University School of Medicine, Cardiff, United Kingdom; and [8]Department of Pediatrics, Ehime University Graduate School of Medicine, Ehime, Japan

Aurora kinase A (AURKA) is overexpressed in leukemias. Previously, we demonstrated that AURKA-specific CD8$^+$ T cells specifically and selectively lysed leukemia cells, indicating that AURKA is an excellent target for immunotherapy. In this study, we examined the feasibility of adoptive therapy using redirected T cells expressing an HLA-A*0201–restricted AURKA$_{207-215}$-specific T-cell receptor (TCR). Retrovirally transduced T cells recognized relevant peptide-pulsed but not control target cells. Furthermore, TCR-redirected CD8$^+$ T cells lysed AURKA-overexpressing human leukemic cells in an HLA-A*0201–restricted manner, but did not kill HLA-A*0201$^+$ normal cells, including hematopoietic progenitors. In addition, AURKA$_{207-215}$-specific *TCR*-transduced CD4$^+$ T cells displayed target-responsive Th1 cytokine production. Finally, AURKA$_{207-215}$-specific *TCR*-transduced CD8$^+$ T cells displayed antileukemia efficacy in a xenograft mouse model. Collectively, these data demonstrate the feasibility of redirected T cell–based AURKA-specific immunotherapy for the treatment of human leukemia. (*Blood*. 2012;119(2):368-376)

Introduction

Aurora kinase A (AURKA) is a member of the serine-threonine kinase family that regulates mitotic cell division from G_2 through to M phase of the cell cycle.[1] The *AURKA* gene maps to chromosome region 20q13.2. AURKA is expressed at low levels in normal cells, including dividing cells, and overexpression of AURKA has clear oncogenic potential.[2,3] Indeed, the *AURKA* gene is overexpressed in various types of cancer,[4] including leukemias.[5,6] Furthermore, correlations between the genetic dysregulation of *AURKA* and susceptibility to cancer, disease status, and prognosis have been described.[4] In particular, *AURKA* gene overexpression correlates with genetic instability and poor differentiation of cancer cells.[7,8] As AURKA expression is tightly regulated in normal tissues and overexpression correlates with malignant transformation, small molecular inhibitors have been developed that selectively target this protein in various tumors. A number of such molecules are currently in early phase clinical trials and preliminary data are encouraging.[9-12]

The overexpression of AURKA in cancer cells, but not in normal tissues, makes it an attractive target for tumor immunotherapy. We have previously shown that testis is the only tissue that expresses detectable levels of AURKA, which suggests that this antigen behaves like cancer/testis antigens.[13] Based on these findings, we previously studied the immunotherapeutic potential of AURKA and identified an HLA-A*0201-restricted antigenic nonamer epitope derived from the kinase domain (residues 207-215). The AURKA$_{207-215}$ epitope (YLILEYAPL) was recognized by CD8$^+$ cytotoxic T lymphocytes (CTLs) generated in vitro.[6] Furthermore, leukemic cells endogenously expressing AURKA were killed by these CTLs, indicating that the cognate epitope is naturally processed and presented in the context of HLA-A*0201 at levels sufficient for immunotherapeutic applications. In addition, Kobayashi and colleagues have identified HLA-class II–restricted AURKA-derived pentadecamer epitopes to which they could generate CD4$^+$ helper T cells that expressed antitumor reactivity.[14]

Immunotherapeutic interventions based on tumor antigen-specific *T-cell receptor* (*TCR*) gene transfer to redirect the specificity of other T cells has shown clinical success in patients with advanced melanoma.[15] However, this approach is complicated by several potential problems: (1) on-target adverse events directed against normal tissues, especially when affinity-enhanced TCRs are used[16]; (2) issues related to chain mispairing between the introduced and endogenous *TCR* α/β genes; and (3) off-target adverse events because of inherent cross-reactivity of the introduced TCR.[17] Although various solutions have been explored to minimize TCR chain mispairing, all current approaches have intrinsic limitations. To this end, we have recently developed a unique vector system that simultaneously delivers *siRNA*s, which specifically down-regulate endogenous *TCR* expression, and a *siRNA*-resistant relevant *TCR* construct (si-*TCR* vector).[18] Furthermore, the likelihood of adverse events related to expression of the introduced TCR may be minimized by the selection of tumor-specific antigens or cancer/testis antigens, rather than tumor-associated antigens. Indeed, a recent clinical study reported that redirected T-cell therapy using NY-ESO-1–specific *TCR* gene

Submitted June 11, 2011; accepted October 13, 2011. Prepublished online as *Blood* First Edition paper, October 24, 2011; DOI 10.1182/blood-2011-06-360354.

*K.N. and T.O. contributed equally to this work.

An Inside *Blood* analysis of this article appears at the front of this issue.

The online version of this article contains a data supplement.

The publication costs of this article were defrayed in part by page charge payment. Therefore, and solely to indicate this fact, this article is hereby marked "advertisement" in accordance with 18 USC section 1734.

transfer displayed antitumor efficacy against metastatic melanoma and metastatic synovial cell sarcoma without obvious toxicities mediated by the transferred T cells.[19]

In this study, we examined the antileukemic efficacy and safety of redirected T cells using HLA-A*0201–restricted $AURKA_{207-215}$–specific *TCR* gene transfer both in vitro and in vivo. The data demonstrate the feasibility of this approach for the treatment of human leukemias.

Methods

Cells and cell lines

Approval for this study was obtained from the Institutional Review Board of Ehime University Hospital (Protocol 0909001 and 0909002). Written informed consent was obtained from all patients, healthy volunteers, and parents of cord blood donors in accordance with the Declaration of Helsinki. B-lymphoblastoid cell lines (B-LCLs) were established by transformation of peripheral blood B-lymphocytes with Epstein-Barr virus. GANMO-1 (HLA-$A2^+$), MEG01 (HLA-$A2^-$), MEG01-A2 (*HLA-A*0201* gene-transduced MEG01), OUN-1 (HLA-$A2^-$), and KAZZ (HLA-$A2^-$) leukemia cell lines were cultured in RPMI 1640 with 10% FCS, antibiotics, and L-glutamine. The artificial antigen-presenting cell line C1R-A2 (HLA-$A*0201^+$) was a kind gift from Dr A. John Barrett (National Heart, Lung, and Blood Institute, Bethesda, MD). The Jurkat/MA cell line (kindly provided by Prof Erik Hooijberg, Vrije Universiteit Medisch Centrum, Amsterdam, The Netherlands) is a Jurkat cell subclone that lacks endogenous TCR expression and stably expresses both the human *CD8α* gene (*hCD8α*) and an *NFAT-luciferase* gene construct for the detection of signaling via newly introduced TCRs.[20] PBMCs and bone marrow mononuclear cells (BMMCs) from leukemia patients and healthy volunteers, and cord blood mononuclear cells (CBMCs) from healthy donors, were isolated by density gradient centrifugation and stored in liquid nitrogen until use. $CD34^+$ cells from CBMCs were isolated using $CD34^+$ cell-isolating immunomagnetic beads (Miltenyi Biotec).

Synthetic peptides and HLA-A*0201/peptide tetrameric complexes

The HLA-A*0201–restricted $AURKA_{207-215}$ nonameric peptide (YLILEYAPL) was purchased from Thermo Electron (Greiner Bio-One). Biotin-tagged soluble HLA-A*0201/AURKA monomers were produced as previously described.[21] Fluorochrome-labeled tetrameric complexes were generated by conjugation to streptavidin-PE (Prozyme) at a molar ratio of 4:1.[22] HLA-A*0201 tetramers were also produced with the HIV-1 p17 Gag-derived peptide epitope SL9 (SLYNTVATL, residues 77-85) for control purposes.

Generation of an $AURKA_{207-215}$-specific CTL clone

A novel $AURKA_{207-215}$-specific CTL clone designated AUR-2 was generated as previously described.[23] Briefly, monocyte-derived dendritic cells (Mo-DCs) were generated from $CD14^+$ PBMCs using 10 ng/mL recombinant human IL-4 and 75 ng/mL recombinant human GM-CSF (R&D systems), then matured with 100 U/mL recombinant human TNF-α (Dainippon Pharmaceutical). $CD8^+$ T cells (1×10^5) were stimulated with 10^4 autologous mature $AURKA_{207-215}$ peptide-loaded (10μM) Mo-DCs in a 96-well round-bottomed plate. One week later, the $CD8^+$ T cells were restimulated similarly, and 10 U/mL recombinant human IL-2 (Roche) was added after a further 4 days. Thereafter, $CD8^+$ T cells were restimulated weekly with 10^5 autologous $AURKA_{207-215}$ peptide-pulsed (10μM) PBMCs treated with mitomycin-C (MMC; Kyowa Hakko). Epitope-dependent target cell cytotoxicity was examined using standard ^{51}chromium (^{51}Cr)–release assays.

ELISPOT

ELISPOT assays were conducted as previously described.[22] Briefly, 96-well flat-bottomed MultiScreen-HA plates with a nitrocellulose base (Millipore) were coated overnight at 4°C with 10 μg/mL anti-IFN-γ monoclonal antibody (mAb; R&D Systems). After washing with PBS, cultured $CD8^+$ T cells were stimulated with 5×10^4 $AURKA_{207-215}$ peptide-pulsed (1μM) or unpulsed C1R-A2 cells/well for 20 hours at 37°C in a 5% CO_2 atmosphere. Subsequently, the wells were vigorously washed with PBS/0.05% tween 20 and incubated with polyclonal rabbit anti–IFN-γ Ab (Endogen) for 90 minutes at room temperature. The wells were then washed again and incubated for 90 minutes with peroxidase-conjugated goat anti–rabbit IgG Ab (Zymed). Spots were visualized by the addition of 100 μL substrate, comprising 0.1M sodium acetate buffer (pH 5.0) containing 3-amino-9-ethylcarbazole (Sigma-Aldrich) and 0.015% H_2O_2, for 40 minutes at room temperature and counted under a light microscope.

Cloning of full-length *TCR* α and β chain genes from the AUR-2 CTL clone and retroviral vector construction

Total RNA was extracted from the HLA-A*0201–restricted $AURKA_{207-215}$-specific CTL clone AUR-2 using the FastPure RNA Kit (Takara Bio) according to the manufacturer's instructions. Full-length *TCR* α and β genes were cloned as previously described.[24] Briefly, cDNA was amplified using a 5′-RACE primer and 3′-constant region primers as follows: (1) 5′-TCAGCTGGACCACAGCCGCAGCGT-3′ for TCR Cα; (2) 5′-TCAGAAATCCTTTCTCTTGAC-3′ for TCR Cβ1; and (3) 5′-CTAGCCTCTGGAATCCTTTCTCTT-3′ for TCR Cβ2. The conditions for PCR were: one cycle at 94°C for 3 minutes, followed by 30 cycles at 94°C for 40 seconds, 58°C for 40 seconds and 72°C for 1 minute, with a final extension phase at 72°C for 5 minutes. Each *TCR* α and β chain amplicon was cloned into the pMD20 TA cloning vector (Takara Bio), and sequenced using the BigDye Terminator v3.1 Cycle Sequencing Kit (Applied Biosystems) and an ABI 3730xl sequencer (Applied Biosystems). Full-length *TCR* α and β genes were then cloned into the bicistronic pMS3 retroviral vector, which is a pME1-5 derivative that contains the murine stem cell virus (MSCV) LTR (Takara Bio) in place of the 3′LTR (pMS3-*AURKA-TCR*, Figure 1). Ecotropic retrovirus particles were obtained by transient transfection of HEK293 T cells with the TCR construct and helper plasmids (pGP vector and pE-eco vector; Takara Bio). GaLV-pseudotyped retrovirus particles were obtained by consecutive transfection into PG13 cells. The pMS3-*AURKA-TCR* GaLV-pseudotyped retroviruses were used for AURKA-specific *TCR* α and β gene transduction.

Transduction of $AURKA_{207-215}$-specific *TCR genes*

Jurkat/MA cells and healthy donor T cells were genetically modified to express the AURKA-specific TCR using RetroNectin (Takara Bio) as previously described.[18] Briefly, 1×10^6 healthy donor T cells per well in GT-T503 (Takara Bio) with 5% human serum, 0.2% human albumin, 50 U/mL recombinant human IL-2 (R&D Systems), 5 ng/mL recombinant human IL-7 (R&D Systems), 10 ng/mL recombinant human IL-15 (PeproTech Inc), and 100 ng/mL recombinant human IL-21 (Shenandoah Biotechnology Inc) were added on day 1 to a 24-well culture plate pretreated with antihuman CD3 mAb (BioLegend). Jurkat/MA cells were cultured in IMDM with 8% FCS and 50 μg/mL hygromycin B (Invitrogen). On day 3, cultured T cells or Jurkat/MA cells were transferred on to a retrovirus-preloaded RetroNectin-coated 24-well plate, centrifuged at 2000*g* for 2 hours and rinsed with PBS. Cells were then applied to the retrovirus-preloaded RetroNectin-coated 24-well plate again for the second transduction. AURKA-specific *TCR*-transduced T cells were stimulated weekly with MMC-treated C1R-A2 cells loaded with $AURKA_{207-215}$ peptide (1μM) for further functional experiments.

Flow cytometric analysis

The AUR-2 CTL clone expresses the *TRBV10-3* gene, denoted in IMGT nomenclature.[25] This corresponds to TCR Vβ12 in the Arden nomenclature.[26] Accordingly, anti-TCR Vβ12 mAb was used to detect $AURKA_{207-215}$-specific *TCR*-transduced cells. After 4 to 6 days, transduced cells were analyzed by flow cytometry using anti-TCR Vβ12-FITC (Beckman Coulter), anti-CD8–FITC (BD Biosciences) or anti-CD8–PE (BioLegend), and HLA-A*0201/$AURKA_{207-215}$ tetramer-PE (only with anti-CD8–FITC).

Intracellular expression of Foxp3 and $AURKA_{207-215}$–responsive IFN-γ production by $AURKA_{207-215}$–specific *TCR*-transduced $CD4^+$ T cells were analyzed using anti–Foxp3-PE (e-Bioscience) and anti–IFN-γ–FITC (BD Biosciences). Data were acquired using a FACS Calibur flow cytometer and analyzed with either Cell Quest (BD Biosciences) or FlowJo Version 7.2.2 software (TreeStar Inc).

CFSE dilution assay

To measure epitope-responsive proliferation of $AURKA_{207-215}$–specific *TCR*-transduced $CD8^+$ T cells in the presence or absence of similarly redirected $CD4^+$ T cells, $CD8^+$ T cells were labeled with CFSE (Molecular Probe Inc) as described previously.[27] After 3 days, CFSE dilution within the $CD8^+$ T-cell population was assessed by flow cytometry.

Epitope-responsive luciferase production by $AURKA_{207-215}$–specific *TCR*-transduced Jurkat/MA cells

To verify the functionality of the cloned $AURKA_{207-215}$–specific *TCR* α and β chains, we used the TCR^- Jurkat/MA cell line, which stably expresses *hCD8α* and an *NFAT-luciferase* reporter gene (Jurkat/MA/CD8α/luc), as follows. pMS3-*AURKA-TCR* was retrovirally transduced into Jurkat/MA/CD8α/luc cells. Cells expressing TCR Vβ12 were isolated for functional analysis. Briefly, HLA-A*0201$^+$ B-LCL cells were loaded with titrated doses of $AURKA_{207-215}$ peptide or the irrelevant SL9 peptide (10μM; HIV-1 p17 Gag, residues 77-85) and used to stimulate 8×10^5 *TCR* gene-modified Jurkat/MA/CD8α/luc cells (effector:target ratio 2:1) for 12 hours. The cells were then lysed and subjected to luciferase assay using the PicaGene-Dual-SeaPansy Kit (TOYOinki) according to manufacturer's instructions. Luciferase activity was measured using a Lumicounter700 (MicrotecNition).

IFN-γ secretion assay

$AURKA_{207-215}$–specific *TCR*-transduced $CD4^+$ or $CD8^+$ T cells (5×10^5) were incubated with 10^5 $AURKA_{207-215}$ peptide-pulsed (1μM) or unpulsed C1R-A2 cells for 24 hours. For the inhibition assay, cells were cultured in the presence of either an anti-HLA class I framework mAb (w6/32; ATCC) or a control anti–HLA-DR mAb (L243; ATCC). Cytokine production patterns were assessed using a bead-based immunoassay kit (Becton Dickinson). IFN-γ in the culture supernatant was measured using an ELISA kit (Pierce) according to the manufacturer's instructions. Streptavidin-HRP was used for color development, and luminointensity was measured using IMMUNO-MINI (NJ-2300; Microtec).

Cytotoxicity assay

Standard ^{51}Cr release assays were performed as previously described.[28] Briefly, 10^4 unpulsed or peptide-pulsed target cells were labeled with ^{51}Cr ($Na_2{}^{51}CrO_4$; MP Bio Japan) and incubated at various ratios with effector cells in 200 μL of culture medium in 96-well round-bottomed plates. To assess HLA class I restriction, target cells were incubated with 10 μg/mL w6/32 mAb or the control L243 mAb for 1 hour, then incubated with effector cells for 5 hours. After incubation, 100 μL supernatant was collected from each well to measure ^{51}Cr release. The percentage specific lysis was calculated as: (experimental release cpm − spontaneous release cpm)/(maximal release cpm − spontaneous release cpm) × 100 (%).

Quantitative analysis of *AURKA* mRNA expression

Quantitative real-time PCR (qRT-PCR) for *AURKA* mRNA was performed as described previously.[6] Briefly, total RNA was extracted using an RNeasy Mini Kit (QIAGEN) and cDNA was synthesized. qRT-PCRs for *AURKA* mRNA (Hs00269212_ml) and glyceraldehyde-3-phosphate dehydrogenase (*GAPDH*) mRNA (4326317E) as an internal control were performed using the TaqMan Gene Expression assay (Applied Biosystems) in accordance with the manufacturer's instructions and an ABI Prism 7700 Sequence Detection System (Applied Biosystems). The expression level of *AURKA* mRNA was corrected by reference to that of *GAPDH* mRNA, and the relative amount of *AURKA* mRNA in each sample was calculated by the comparative ΔCt method.

AURKA protein expression analysis by Western blotting

For the analysis of protein expression, Western blotting was performed as described previously.[6] Briefly, cell lysates were subjected to 10% SDS-PAGE (e-PAGEL, ATTO) and blotted onto PVDF membranes (Bio-Rad Laboratories). The blots were incubated first with anti-AURKA mouse mAb (Abcam), then with HRP-conjugated anti–mouse IgG (GE Healthcare). The probed proteins were visualized using an enhanced chemiluminescence system (GE Healthcare). Subsequently, the blotted membranes were stripped and reprobed with anti–β-actin mouse mAb (Sigma-Aldrich) to confirm equivalent protein loading between samples.

Antileukemia effect of $AURKA_{207-215}$–specific *TCR*-transduced T cells in xenograft mouse models

All in vivo experiments were approved by the Ehime University animal care committee. For the Winn assay, 5×10^6 GANMO-1 cells and 2.5×10^7 $AURKA_{207-215}$–specific *TCR* gene-transduced or non–gene-modified $CD8^+$ T cells were inoculated per mouse (n = 4 per group). The cells were suspended in 300 μL PBS and injected subcutaneously into the left flank of NOG mice (Non-Obese Diabetic/Severe Combined Immuno-Deficiency/IL-2 receptor γ-chain allelic mutation; *NOD*/Shi-*scid*/IL-2R γ^{null})[29] aged 5-6 weeks (Central Institute for Experimental Animals). Mice were subsequently injected intravenously with either 5×10^6 $AURKA_{207-215}$–specific *TCR* gene-modified cells, AUR-2 cells or unmodified $CD8^+$ T cells, as per the initial inoculation, on a weekly basis for a total of 5 infusions. Tumor size was measured every 5 days until the mice died or were euthanized because of tumor progression.

For adoptive transfer experiments, NOG mice aged 9 weeks were similarly inoculated with 5×10^6 of GANMO-1 cells. Intravenous administration of either 5×10^6 $AURKA_{207-215}$–specific *TCR* gene-transduced or non–gene-modified $CD8^+$ T cells commenced on the same day (day 0), and was continued on a weekly basis thereafter until the mice died or were euthanized because of tumor progression.

Statistical analysis

The paired *t* test was used to assess differences between groups; a *P* value $< .05$ was considered significant.

Results

Generation of a novel HLA-A*0201–restricted $AURKA_{207-215}$–specific CTL clone (AUR-2) and retroviral expression of the full-length *TCR* α and β genes

Characteristics of the newly established HLA-A*0201-restricted $AURKA_{207-215}$–specific CTL clone (AUR-2) are shown in Figure 1. AUR-2 was stained uniformly with the HLA-A*0201/$AURKA_{207-215}$ tetramer, but not with the irrelevant HLA-A*0201/Gag_{77-85} tetramer (Figure 1A). In cytotoxicity assays, AUR-2 displayed moderate levels of functional sensitivity in response to cognate peptide (Figure 1B). Epitope-dependent production of IFN-γ was confirmed in ELISPOT assays (Figure 1C). Peptide specificity and HLA restriction were further demonstrated in cytotoxicity assays with different target cells (Figure 1D). In addition, AUR-2 lysed the HLA-A*0201$^+$ leukemia cell line GANMO-1, which overexpresses *AURKA* mRNA, but not the HLA-A*0201$^-$ negative cell lines MEG01 and K562, both of which also express *AURKA* mRNA at high levels (Figure 1E). The rearranged *TCR* α and β genes of AUR-2 were sequenced and found to comprise the germ line gene segments *TRAV3/TRAJ20/TRAC* and *TRBV10-3/TRBJ1-1/TRBC1*, respectively; both full-length genes were cloned into a novel bicistronic retroviral vector (Figure 1F).

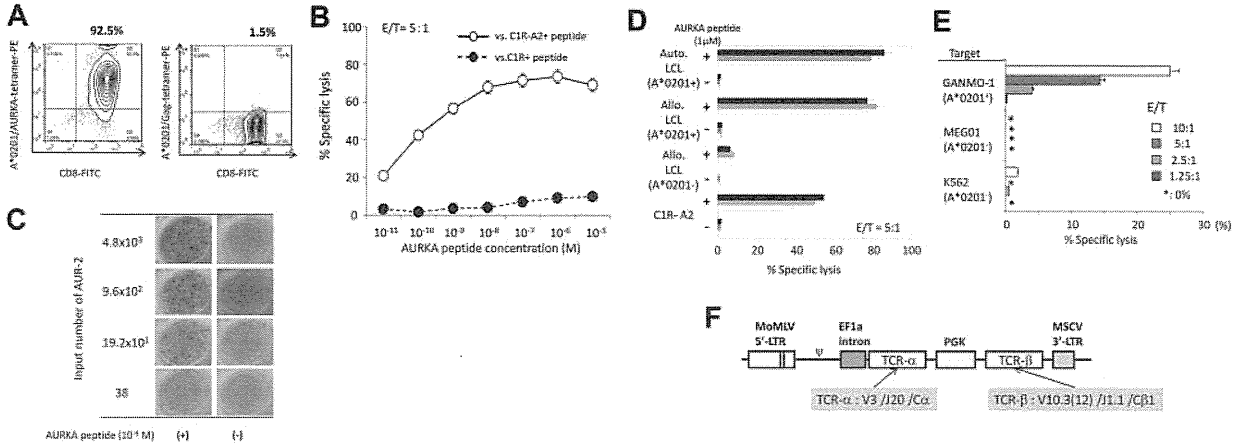

Figure 1. Characteristics of the AURKA$_{207\text{-}215}$–specific CTL clone AUR-2. (A) Representative flow cytometry plots showing staining of AUR-2 with the HLA-A*0201/AURKA$_{207\text{-}215}$ tetramer (left) and the irrelevant HLA-A*0201/Gag$_{77\text{-}85}$ tetramer (negative control; right). (B) The cyotoxic activity of AUR-2 was measured in ^{51}Cr-release assays against C1R-A2 or C1R (negative control) cells loaded with a range of AURKA$_{207\text{-}215}$ peptide concentrations as indicated. E/T indicates effector:target ratio. (C) IFN-γ ELISPOT assays were conducted using C1R-A2 target cells loaded with 1 μM AURKA$_{207\text{-}215}$ peptide and AUR-2 CTL at different input numbers as shown. (D) ^{51}Cr-release assays were conducted using AUR-2 CTL with unpulsed or AURKA$_{207\text{-}215}$ peptide-pulsed (1 μM) HLA-A*0201$^+$ autologous or allogeneic B-LCLs, C1R-A2 cells or HLA-A*0201$^-$ allogeneic B-LCLs as indicated. E/T indicates effector:target ratio. (E) The cytotoxic activity of AUR-2 CTL against the indicated leukemia cell lines was measured in ^{51}Cr-release assays. GANMO-1, HLA-A*0201$^+$; MEG01 and K562, HLA-A*0201$^-$. Expression of *AURKA* mRNA and AURKA protein in these leukemia cell lines is shown in supplemental Figure 2. E/T indicates effector:target ratio. (F) Construction of a novel retroviral vector encoding full-length AURKA–specific *TCR* α and β genes derived from AUR-2. MoMLV indicates Moloney murine leukemia virus; LTR, long terminal repeat; EF1a, elongation factor 1a; PGK, phosphoglycerate kinase promoter; and MSCV, murine stem cell virus. Error bars represent SDs.

Functional reconstitution of the AURKA$_{207\text{-}215}$–specific TCR heterodimer in Jurkat/MA cells

To validate the functionality of the cloned *TCR* genes, both chains were expressed in the TCR$^-$ cell line Jurkat/MA/CD8α/luc, which contains a luciferase reporter gene to monitor TCR signaling (Figure 2A). AUR-2*TCR*–transduced, Vβ12-selected Jurkat/MA/CD8α/luc cells (Figure 2B) were incubated with C1R-A2 cells pulsed with a range of AURKA$_{207\text{-}215}$ peptide concentrations, then assayed for luciferase activity. The *TCR* gene-modified Jurkat/MA/CD8α/luc cells produced luciferase in response to stimulation with AURKA$_{207\text{-}215}$ peptide-loaded C1R-A2 cells in a dose-dependent manner (Figure 2C). Compared with the parental AUR-2 CTL clone (Figure 1B), the *TCR*-transduced Jurkat/MA cells displayed low levels of peptide sensitivity. To address this functional discrepancy, we assessed cell-surface expression of TCR α/β, CD3, CD8α, CD11a, and CD28 (supplemental Figure 1, available on the *Blood* Web site; see the Supplemental Materials link at the top of the online article). The *TCR*-transduced Jurkat/MA cells expressed lower surface levels of TCR α/β, CD3 and CD8α compared with both similarly activated normal CD8$^+$ T cells and the parental AUR-2 CTL clone. Furthermore, CD11a and CD28 were almost absent from the transfectant cells. These findings may explain the observed differences in functional sensitivity between AUR-2 *TCR*-transduced Jurkat/MA cells and the parental CTL clone.

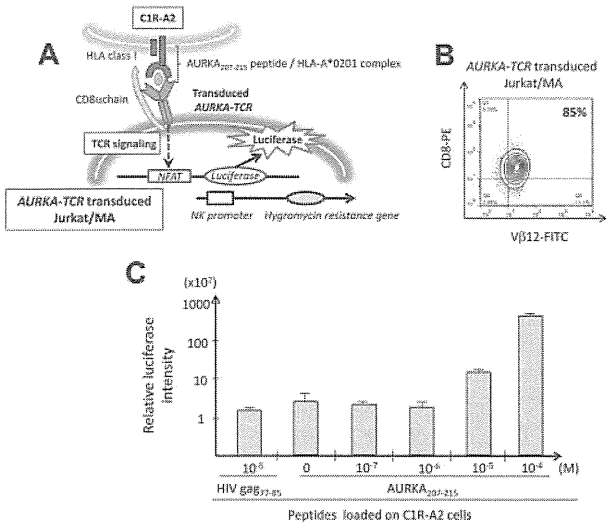

Figure 2. Functional retroviral expression of the AURKA$_{207\text{-}215}$–specific TCR. (A) Schematic representation of the luciferase assay using AURKA$_{207\text{-}215}$–specific *TCR*-transduced Jurkat/MA cells. NFAT indicates nuclear factor activated T cells; and NK, natural killer. (B) AURKA$_{207\text{-}215}$–specific *TCR*-transduced Jurkat/MA cells express Vβ12 but label poorly with cognate tetramer (data not shown), probably because of the low levels of surface CD8α expression. (C) AURKA$_{207\text{-}215}$–specific *TCR*-transduced Jurkat/MA cells were stimulated with peptide-pulsed C1R-A2 cells as shown and subjected to luciferase assay. Error bars represent SDs.

AURKA$_{207\text{-}215}$–specific *TCR* gene-transduced CD8$^+$ T cells exert antileukemia reactivity in vitro

Next, the AURKA$_{207\text{-}215}$–specific *TCR* was retrovirally introduced into normal CD8$^+$ T cells. Transduction efficiency determined by Vβ12 staining of *TCR* gene-modified T cells was 50%-70% (data not shown), and 20%-25% of the Vβ12$^+$ cells stained with the HLA-A*0201/AURKA$_{207\text{-}215}$ tetramer (Figure 3A). Isolated Vβ12$^+$ AURKA$_{207\text{-}215}$–specific *TCR* gene-transduced CD8$^+$ T cells displayed similar antigen sensitivity to the parental AUR-2 CTL clone (Figure 3B-C). Notably, however, the AURKA$_{207\text{-}215}$–specific *TCR* transductants produced higher quantities of IFN-γ in response to the same peptide-pulsed C1R-A2 targets (Figure 3C). On the basis of these observations, further experiments were carried out using these AURKA$_{207\text{-}215}$–specific *TCR* gene transfectants.

AURKA$_{207\text{-}215}$–specific *TCR*-transduced CD8$^+$ T cells displayed HLA class I–restricted, peptide-dependent IFN-γ production (Figure 3D), and target epitope–specific cytotoxic activity (Figure 3E). Furthermore, these redirected CD8$^+$ T cells selectively lysed the HLA-A*0201$^+$ leukemia cell line GANMO-1, which overexpresses AURKA, but not the HLA-A*0201$^-$ leukemia cell lines, MEG01, KAZZ, and OUN-1, which also overexpress AURKA (Figure 4A, supplemental Figure 2). In contrast,